A simple spatial navigation paradigm in aging mice connects heterogeneous behavioral phenotypes with neuropathology and Alzheimer's disease

Joo Young Park

A thesis

submitted in partial fulfillment of the

requirements for the degree of

Master of Science

University of Washington

2024

Committee:

Warren Ladiges

Thea Brabb

Brian Iritani

Derek Huffman

Program Authorized to Offer Degree:

Comparative Medicine

University of Washington

Abstract

A simple spatial navigation paradigm in aging mice connects heterogeneous behavioral phenotypes with neuropathology and Alzheimer's disease

Joo Young Park

Chair of the Supervisory Committee:
Warren Ladiges
Department of Comparative Medicine

Aging of the brain affects everyone, but some develop signs and symptoms, such as a decline in cognitive function, more quickly than others. Spatial navigation confusion and memory deficits with increasing age may be one of the first indicators of more serious cognitive impairment associated with Alzheimer's disease (AD). This project was designed to evaluate a spatial navigation learning task coined Boxmaze to predict resistance to AD progression. C57BL/6 female and male mice, 20 months of age, were tested for cognition using the Boxmaze, and then intravenously administered AAV-Aβ42 and AAV-pTau, or an AAV sham vector and followed for two months. Mice were then tested in the Y-maze and retested in the Boxmaze, followed by euthanasia and collection of brain tissues for formalin-fixation and immunohistochemistry using antibodies specific for neuropathology associated aging and AD. A spatial learning index, reflecting individual learning rates, was developed to measure distinctions in cognitive decline. Behavioral data showed that mice had differing susceptibilities to further cognitive decline with correlation of pre-AAV learning index and post-AAV learning index. Cognitive impairment phenotypes were not associated with neuropathology or other aging markers in the brain. Data from this project suggest that the Boxmaze spatial learning index could potentially predict early signs of learning impairment and screen for indicators of resistance or susceptibility to AD.

Keywords: Alzheimer's disease, Cognitive Impairment, Boxmaze, Aging, Resiliency

Acknowledgements

I am extremely grateful to my committee members, Dr. Thea Brabb, Dr. Brian Iritani, and Dr. Derek Huffman, for their invaluable patience, feedback, and expertise. I would like to thank Dr. Warren Ladiges for his unwavering support and direction throughout the study refinement process, and believing in my thesis no matter the number of times I pivoted.

A big thank you to James Buenfil for his significant contribution to the project's biostatistics effort.

Thank you to Dr. Ruby Sue Mangalindan, John Morton, and Dr. Soroosh Fatemie-Nainie for their constant attention and consideration to the logistical success of my project.

Major thanks to Devika Gandhay who helped with the live mouse experiments, and Juliana Moreno, Katherine Pham, and Elizabeth Bae who helped with IHC, and Jackson Wezeman and Chloe Johnson for their help with mice injections, and Addison Keeley and Manuela Rosenfeld for their help with necropsies, and Katherine Qianpei He for her much appreciated kind moral support.

Specialty VetPath (SVP) cut and embedded tissues and created slides for IHC. UW Alzheimer's Disease Research Center (ADRC) Neuropathology Histology Lab provided important IHC samples.

Dedication

I dedicate my work to my dad and brothers whose guidance and support inspired and instilled in me a love for learning, and continue to lift me up.

Table of Contents

Introduction

Neurodegenerative diseases such as Alzheimer's Disease (AD) commonly develop in older stages of life in a progressive manner accompanying memory impairments and cognitive decline. Recognizable neuropathology traits of AD remark an accumulation of amyloid β and phosphorylated tau in the brain, although historically both have not served as effective drug targets. The precursor steps that eventually lead to elevated levels of amyloid β proteins and AD diagnosis present as forgetfulness and impaired decision making in clinical mild cognitive impairment (MCI), and spatial navigation deficits **(Zanco et al., 2018).** Given that there is still no curative treatment for AD, reducing the risk in older populations is essential to slow the surge in the prevalence of AD and to reduce economic burdens **(Zekry et al., 2002; Mangialasche et al., 2012).** Because AD develops in a cumulative manner in older people, characterizing early signs of AD disease progression could point to important indicators of developing more serious cognitive impairment and neurodegeneration.

AD's brain aging process include decline in attention, memory, executive function, and visuospatial abilities. Given known patterns and motifs of AD's phenotypic behavior and molecular pathways, there is incentive to discover potential interconnected interventions that may help mitigate the cognitive progression of AD or subdue it's neuropathology. However, heterogeneity of the older population suggests existence of subsets of individuals who share certain brain molecular features and respond differently to AD risk factors. A recent study using RNA sequence profiles of participants in longitudinal studies of cognitive aging showed evidence of two meta-clusters that differ primarily in their trajectories of cognitive decline, thought to be due to a greater impact of tau pathology on neuronal chromatin architecture and to broader brain changes **(Lee et al., 2023).** These findings suggest that different pathways of

aging in the brain can enhance the effect of risk factors for dementia in older people or provide protective effects depending on the transcriptomic profile. In a second study, mapping transcriptomic changes of endothelial cells in the human hippocampus showed alterations in cell adhesion molecules, increased inflammation, brain-insulin resistance, lipidic alterations, and changes in the extracellular matrix in an older group with age-related cognitive impairment (ARCI), less changes in an older group without ARCI, and no changes in a younger group **(Guebel et al., 2022).** This data also indicates that older individuals differ in expression of aging pathways that provide either protection or increased susceptibility to more severe cognitive impairment and most likely AD.

A study showed performance on spatial navigation assessing two-dimensional Floor Maze Test (FMT) on human patients (**Sanders et al., 2008**), worsened with increasing severity of cognitive impairment determined by cognitive function tests that categorized subjects into distinguishable subjective cognitive impairment, MCI, or mild AD **(Tangen et al., 2015)**. Their evidence also suggested performance on the FMT was significantly associated with executive function, and that conventional cognitive function testing methods do not always reveal impairments of spatial navigation. More recently, **Placido et al.** found spatial navigation tests involving walking in real environments may better recognize cognitive impairment levels than other object-based cognitive screening tests **(Placido et al., 2021).**

Considered the golden standard for mouse spatial memory assessment, the Morris Water Maze (MWM) is a comparative behavioral learning and memory task with various interpretation methods. The MWM has shown cognition differences between young and aged animals and further that there were apparent individual differences in aged rodents regarding learning impairment **(Gage, Dunnet & Bjorklund, 1984; Gallagher & Burwell, 1989; Rapp, Rosenberg & Gallagher, 1987)**. Some aged animals were able to perform on the spatial task

as proficiently as young counterparts. These findings allude to the concept that cognitive impairment in an aging background may develop at different rates. Another implication may be that individuals have differing susceptibility or resistance to ARCI onset and progression.

Based on these observations, it may be possible to assess ways that cognitive function measures could predict the emergence of AD factors and provide characterization on ARCI development in a progressive manner. Further, the prediction system could help correlate individual differences in cognitive decline with other neurobiological features or other systemic pathological markers **(Jiang et al., 2022).**

Addressing this objective, a spatial learning index, whose concept was first adapted for use in the MWM, was developed to provide a scored variable on a continuous scale for measuring individual differences in the effects of cognition. The Boxmaze mouse spatial navigation task assay yields productive quantitative data interpretation from a single day procedure to measure cognitive performance. The workflow that will be described is a modified mathematical method altered from a version of the learning index development by pioneers of the MWM **(Gallagher & Burwell, 1993)**, that validates that the spatial learning index formulation can be effectively applied to the Boxmaze task on testing cognitive decline. The results were then overlaid with other phenotypic parameters and molecular AD factors involved in age related cognitive impairment via the Y-maze assay, white blood cell counts, and immunohistochemistry (IHC). Using C57BL/6 mice as a translational model to observe AD development phenotypes and neuropathology, the hypothesis of this thesis project is: **differences in response to AD neuropathology features are determined by age-related processes in the brain**.

Materials and Methods

Mice. 20-month old C57BL/6 male and female mice from the National Institute on Aging Aged Rodent Colony were housed in a 14:10 light cycle pathogen-free facility with diet and water ad libitum and received safe handling procedures with an approved UW IACUC protocol.

Boxmaze. 20 male and 19 female 20-month-old C57BL/6J mice from the NIA Aged Rodent Colony underwent the single-day Boxmaze spatial navigation learning test that measures visuospatial cognitive ability and cue-dependent learning **(Darvas et al., 2019).** Mice were subjected to 4 trials of attempts to escape the box-like arena fit with 2 holes equidistantly on each of the 4 walls. Plastic PVC caps closed off all holes but one, which led to an open rest cage through a pipe of the same material. Mice are given a maximum of 120 seconds to explore and escape the maze arena, 30 seconds to rest in the rest-cage, and 1 minute of rest in the home-cage before the subsequent trial. To minimize confounding pheromone variables of different mice in the same testing arena, handler role assignments were kept constant and inter-trial clean up protocol was enforced. Observations were recorded for anxious rearing behavior, latencies for the mice to find the escape hole, and number of attempts into hole entrances, labeled 1 through 8. In this project, Boxmaze performance was the cornerstone assessment of cognitive function.

Adeno-associated virus (AAV)-mediated viral vector delivery of AD components. A week after initial Boxmaze testing, the mice were subjected to retro-orbital viral vector transductions to assess enhancement or attenuation effect of the penetrance of AAV-mediated neuropathological features of either an AAV-Aβ42 and pTauP301L (each 10^{12} vg per concoction) vector (AAV-AD), or an AAV-mCherry (AAV-Sham) vector for control units, at a 14:6 ratio respectively for female mice and a 12:8 ratio respectively for male mice. The encoded

vectors were an AAV9-PHP.eB serotype introduced intravenously to the mouse retro-orbital plexus to facilitate transduction of cDNA genetic material coding for the target peptides to the neural system causing synaptic alterations analogous to those found in human amyloid deposition of dementia and the presence of phosphorylated Taupathy **(Forner et al., 2019, Lawlor et al., 2007, Jang et al., 2022, Cook et al., 2015).** The AAV PHP. eB variant derived from AAV9, with a tropism for neuronal cells, was employed due to its ability to engage with the endothelial LY6A receptor in C57BL/6 mice and breach the blood-brain barrier (BBB). In contrast, certain strains of mice carry variants of the LY6A receptor incompatible for the passage of AAV PHP.eB through the BBB **(Huang et al., 2019).** Additionally, the sequence constructs contained a CAG enhancer promoter and CMV-β Actin immunoglobulin to drive expression, alongside a reporter gene sequence encoding for GFP. The SHAM control infusions encoded for the mCherry reporter regulated by the synapsin promoter-controlled delivery of the hM4d receptor, which remained inactive by design in this study.

Post-AAV assays. After 2 months of monitoring and exogenous viral amplification, the mice underwent Y-maze assay and another round of Boxmaze in anticipation of changes in behavioral patterns associated with AD cognitive impairment. Additionally, to compare the immunological state of the mice groups and assess chronic stress by vector-type, before viral AD neuropathology introduction and at the end point of the study 2 months after, total white blood cell (WBC), neutrophil, lymphocyte, and monocyte counts were taken using either a Turk solution and hemocytometer or Wright-Giemsa stained blood smear methodology. The two timepoints will be called ‘pre-AAV’ testing and ‘post-AAV’ testing for this study. Post-vector, mice were euthanized by CO2, cervically dislocated, and their brain tissues were isolated for formalin-fixed for IHC analyses. This approach allowed for the investigation of neuronal factors associated with brain aging processes at varying baseline levels of cognitive impairment in mice that will more fully characterize neurotropic molecular and cellular events occurring with

increasing age and determine how changes may influence resistance to AD disease development. Post-AAV, the weights of all mice were monitored on a weekly basis.

Immunohistochemistry. After 2 months of Aβ42 and Tau tangle growth, the mice were euthanized and tissues were fixed in formalin. The fixed tissues were paraffin embedded into blocks by Specialty VetPath (SVP) services (Seattle, WA) and cut onto charged slides for IHC analysis. The aging parameter antibodies of interest identified were MCP-1 to measure inflammation and immune cell regulation, GFP signaling reporter gene in the AD associated Aβ42 construct, γH2Ax to measure DNA damage and repair in DNA double stranded breaks, PSD95 to measure synapse assembly and plasticity, and IL-6 for immune defense reaction examination. IHC on 3 key markers of AD (6E10, IBA-1, AT8) was done by the UW Alzheimer's Disease Research Center (ADRC) Neuropathology Histology Lab. Slides were mounted and staining images were taken at 20x magnification. Images were processed through Qupath open source digital pathology imaging software (ver. 0.5.1) by annotation measurements of DAB OD mean intensity feature calculated entire pixel tile creations.

Statistics.

K-means clustering used multi-dimensional phenotypic data applicable to Boxmaze, shown in **Supplementary Table 1**, for separating non-hierarchical observations into k numbers of groups by minimizing Euclidean distances of variances between points and the nearest centroid of the assigned groups.

For non-gaussian data comparing pre-AAV and post-AAV conditions, the significance tests used differences in results median values from each vector-type cohort, which were assessed by Wilcoxon matched-pairs signed-rank test. For non-parametric data with independent sample

variables, Mann-Whitney test or Krustal-Wallis H test followed by Dunn's multiple post-hoc comparisons, was used depending on whether comparison was made between 2 groups or more groups. Normality of data distribution was assessed using the Shapiro-Wilk test. For parametric data such as the results from IHC analyses and WBC measurements, 2-way or 3-way ANOVA was implemented depending on whether comparison was made between 2 groups or more groups. These tests were performed by Graphpad Prism (ver. 8.0) and scientific significance was indicated at p=0.05 or 95% chance the null hypothesis can be rejected with difference between cohorts not due to random chance.

According to bootstrapped distribution, no existence of normality in data was determined in learning index scores. Spearman rank correlation was used over Pearson's correlation because it is more robust to outliers, except in IHC correlation analyses where

Values given in the multivariate regression model analyses are indicated as mean ± SEM. T-tests for significance in the multivariate regression model investigations were calculated in R statistical computing environment (ver. 4.3.2).

The pre-AAV Boxmaze data contained one distinct mouse performance outlier **('MCI 4-LB' in Supplementary Table 2**) which was removed from all analyses. With Boxmaze trial times of 120 seconds for all 3 last trials, the trajectory of the outlier data was deemed illogical in assessing cognition. Performance noncompliant to study design indices perhaps points to unknown or uncontrollable environmental variables (excess anxiety, stress, pheromone cues, etc.), not measurable in this study that will not challenge interpretation.

Results

Heterogeneity exists in cognitive impairment in aged C57BL/6 inbred mice.

Performance showing decreased latencies in a maze, across a series of trials do not necessarily convey memory retention and learning acquisition. Mice display a spectrum of learning rates in an aging brain background, similar to humans. **Figure 1** shows differences in pre-AAV spatial learning performance determined by Boxmaze trial times between individual mice are wide-ranging. Bringing this notion into data modeling, what types of informational system applies to cognitive data fixed with natural phenotypic variability?

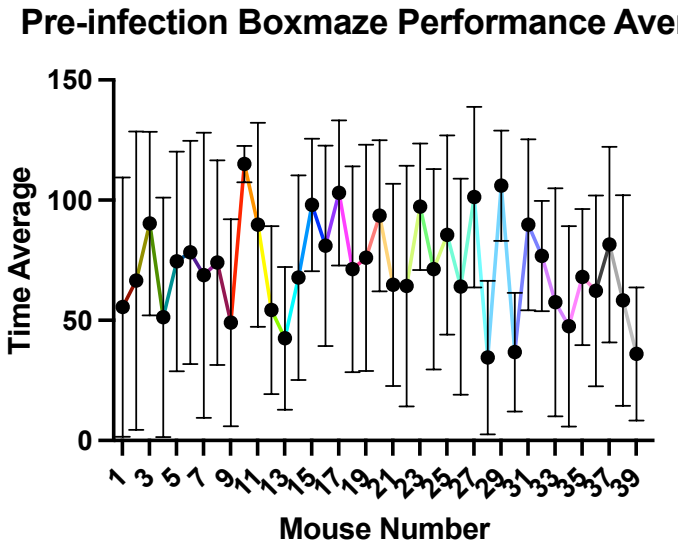

Figure 1. Line chart showing each mouse's average performance through all 4 trials of Boxmaze, with lines indicating range. There is variability in mouse speeds in completing Boxmaze learning assay.

Kernel density estimation is a non-parametric way to estimate the distribution of a random variable given samples from that distribution. Kernel density estimates of pre-AAV Boxmaze trial times revealed no large visual difference between male and female mice probability density functions through the trial times, except for the fourth trial where males tended to have more evenly spread out probability densities of Boxmaze times and females displayed probability densities peaking around the 50 second mark (**Figure 2 A, B, C, D**). The lack of consistency in kernel density in the fourth trial may indicate a sex-difference in cognitive fatigue or fading

attention and increased disinterest in accomplishing the learning task trial. Perhaps this inconsistency indicates the fourth trial is not valuable in assessing overall spatial learning, something downstream Boxmaze paradigms may come to consider.

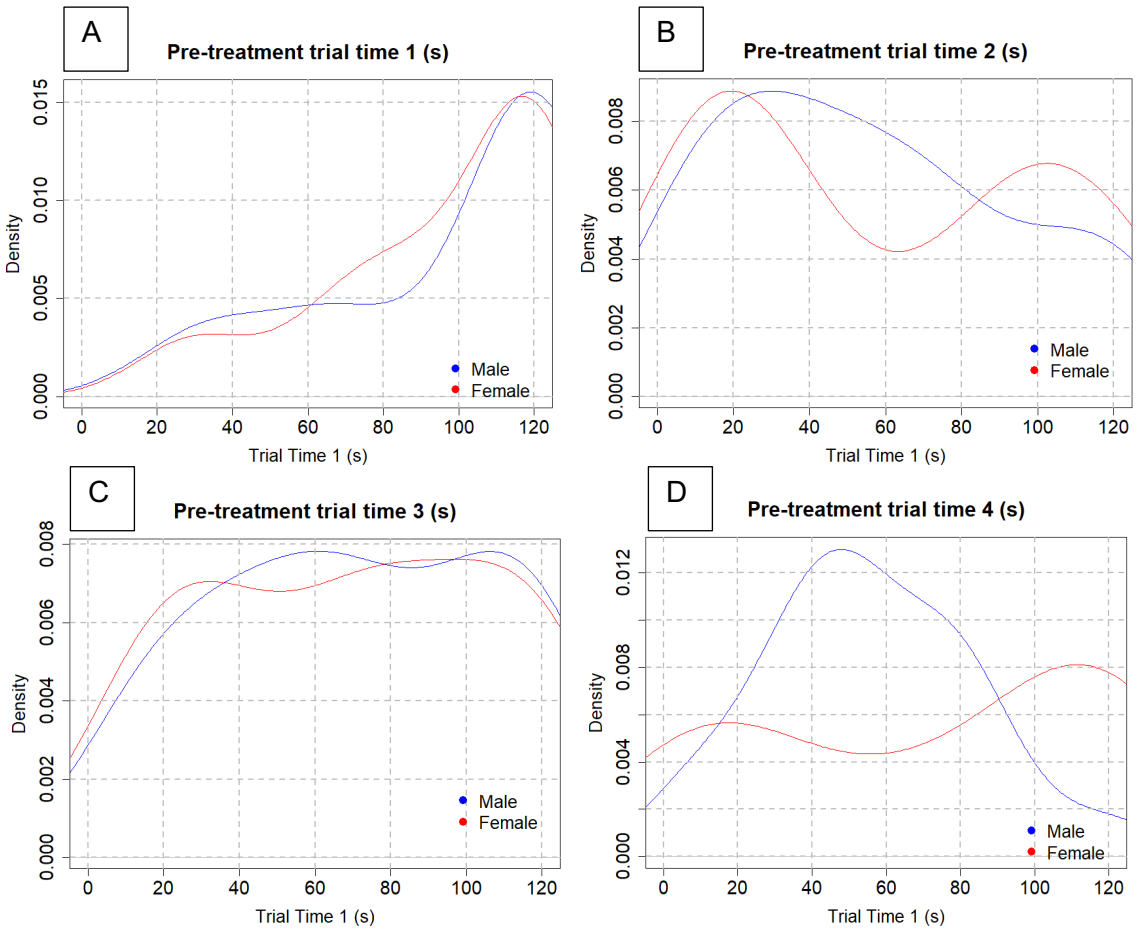

Figure 2. Kernel density estimates of the distributions of the mice times for pre-AAV Boxmaze trials **A.** 1, **B.** 2, **C.** 3, **D.** 4, colored by sex of mice. These kernel density estimate plots can describe likelihood of Boxmaze time performance taking on a particular value and identify concentrations in probability density outcomes. N=19-20 per sex.

Phenotypic parameters of C57BL/6 mice involved in Boxmaze performance do not display obvious clustering behavior by PCA.

Clustering analysis can be used when looking to find similarities in a quantitative dataset of many variables. Considering the Boxmaze assay captures many phenotypic parameters and that Boxmaze performance considers these parameters when evaluating place learning,

unsupervised k-means clustering was applied on mice behavioral features during Boxmaze to separate mice performance into 2 groups of cognition levels a priori, under the hypothesis that general AD cognitive trends can be differed consisting of 2 subgroups. K-means clustering works to identify relationships among observations by grouping data into clusters based on the Euclidean similarity of input variables' data points. The Boxmaze input variables used were 'weight', 'Trial 1', 'Trial 2', 'Trial 3', 'Trial 4', 'Hole Entry Attempts', 'Pellets', and 'Grooming Behavior'. First, with Anaconda navigator Jupyter notebook (ver. 2.5.3), 'scikit-learn' package's (**Pedregosa et al., 2011**) Sklearn.preprocessing library's 'StandardScalar' function normalized the raw Boxmaze observations so that each variable feature had a mean of 0 and a standard deviation of 1, ensuring all data was scaled to the same dimension. Then, K-means clustering was applied by 'Sklearn.cluster' library to examine correlations between variables, and indicate differences in the measured variables between groups. The K-means clusters, where each observation belong to the cluster with the nearest mean decided by iteration to reduce the variance within clusters and maximize the variance between clusters, classified each mouse into 2 groups.

To best observe the separation and distinctive characteristics of the k=2 clusters in a meaningful way making it easier to visualize and interpret, a Boxmaze measurement multi-dimensional dataset (**Supplementary Table 1**) was plotted on 2 principal components. An exploratory data analysis approach was taken to identify underlying patterns and relationships in the K-means classified complex dataset. By this lower-dimensional space visualization, how well the clusters formed by K-means are separated was assessed. PCA also reveals natural classifications or subgroups sharing common features or underlying structures that aren't apparent in higher-dimensional space, so PCA groupings could be juxtaposed with K-means clusters. Each point represents phenotypic summary indices of one mouse and groups of points with large overlaps indicate there are none or only small differences in the measured variables

between groups. The visualization in **Figure 3** illustrates the separation layout of the observations in clusters formed by K-means in the reduced-dimensional space.

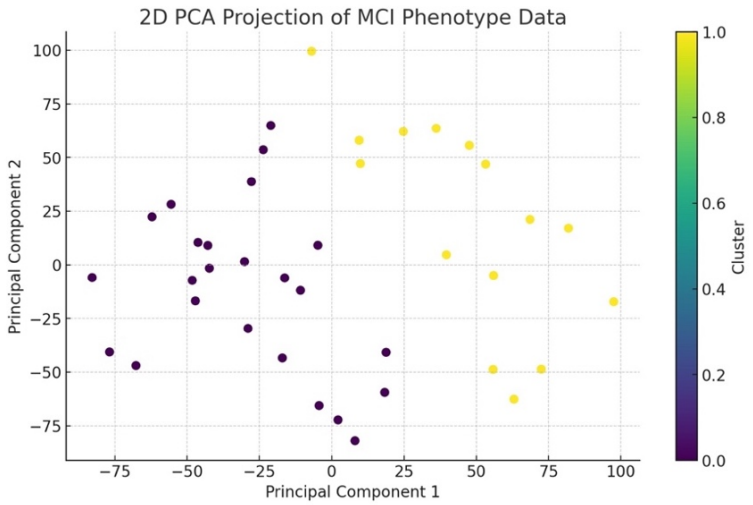

Figure 3. The above visualization shows the pre-AAV raw Boxmaze phenotype data projected onto two dimensions using PCA, with the data points indicating one mouse dataset and colored according to their assigned cluster. The clusters were determined based on all phenotypic variables in the Boxmaze dataset under K-means parameters. N=39.

Since PCA identifies the axes that maximize the variance in the data, it was imperative to place multidimensional data on the StandardScalar standardization method before applying PCA, ensuring each feature contributes equally to the determination of the principal components and that the PCA isn't biased toward the features with larger magnitudes (**Figure 4**). Now with standardization so data are measured in the same scale, principal components are shown with a pattern due to the actual structure of the data not merely because of the scale of certain variables. However, as seen in **Figure 4**, pre-AAV Boxmaze data did not follow explicit spatial grouping patterns according to clustering of K-means. Though K-means may apply well for 2 naturally occurring datasets, it may be too simplistic for any continuous datasets with overlapping patterns or complex datasets such as cognitive impairment measured by Boxmaze phenotypic data **(Supplemental Figure 1)**. The PCA plots show there is no obvious separation into groups of the pre-AAV Boxmaze data.

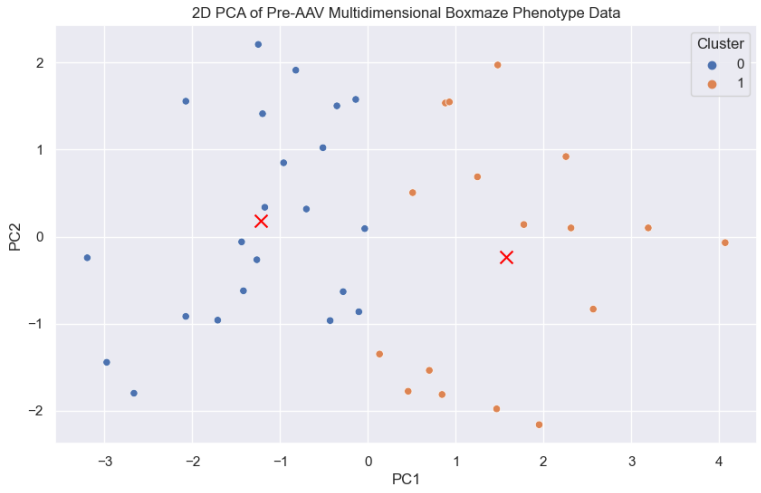

Figure 4. Standardized multi-dimensional pre-AAV Boxmaze phenotype data plotted on a two-dimensional PCA, colored by K-means cluster when k=2. Cluster centroids are indicated with a red X. N=39.

	PC1	PC2
Weight	-0.002789	-0.004106
Trial 1	0.166658	0.430237
Trial 2	0.619416	0.563450
Trial 3	0.521001	-0.389301
Trial 4	0.372184	-0.587797
Average	0.419815	0.004147
Hole Entry Attempts	0.048011	-0.017821
Pellets	0.005383	-0.002721

Table 1. PCA loading chart indicates that Trial 2 exerts the greatest impact on principal components. In PCA, loadings serve as the coefficients that, when applied to each standardized original variable, construct the principal components. These loadings quantify the degree of influence each original variable has on a principal component, with the loading sign (+ or -) denoting the direction of the association between the variable and the principal component.

Learning rates in C57BL/6 mice do not display significant clustering behavior by inter-trial Boxmaze comparisons.

To see potential clusters between trials, plots of the times from Boxmaze trials 2, 3, and 4 were made against each other, with sex indicated by symbol, shown in **Figure 5 A, B, C**. If a mouse sped up from the initial trial to the subsequent trial, the point is below the blue line. If the mouse slowed down, then the point is above the line. There was no thorough undisguised evidence of clustered data points showing separation of mice learning rates based on the speed of trial-to-trial performance. Clustering of data points would indicate presence of groups of mice with

similar learning rate levels, whether they be advanced resilience or aged susceptibility to cognitive impairment between subsequent encounters with the maze.

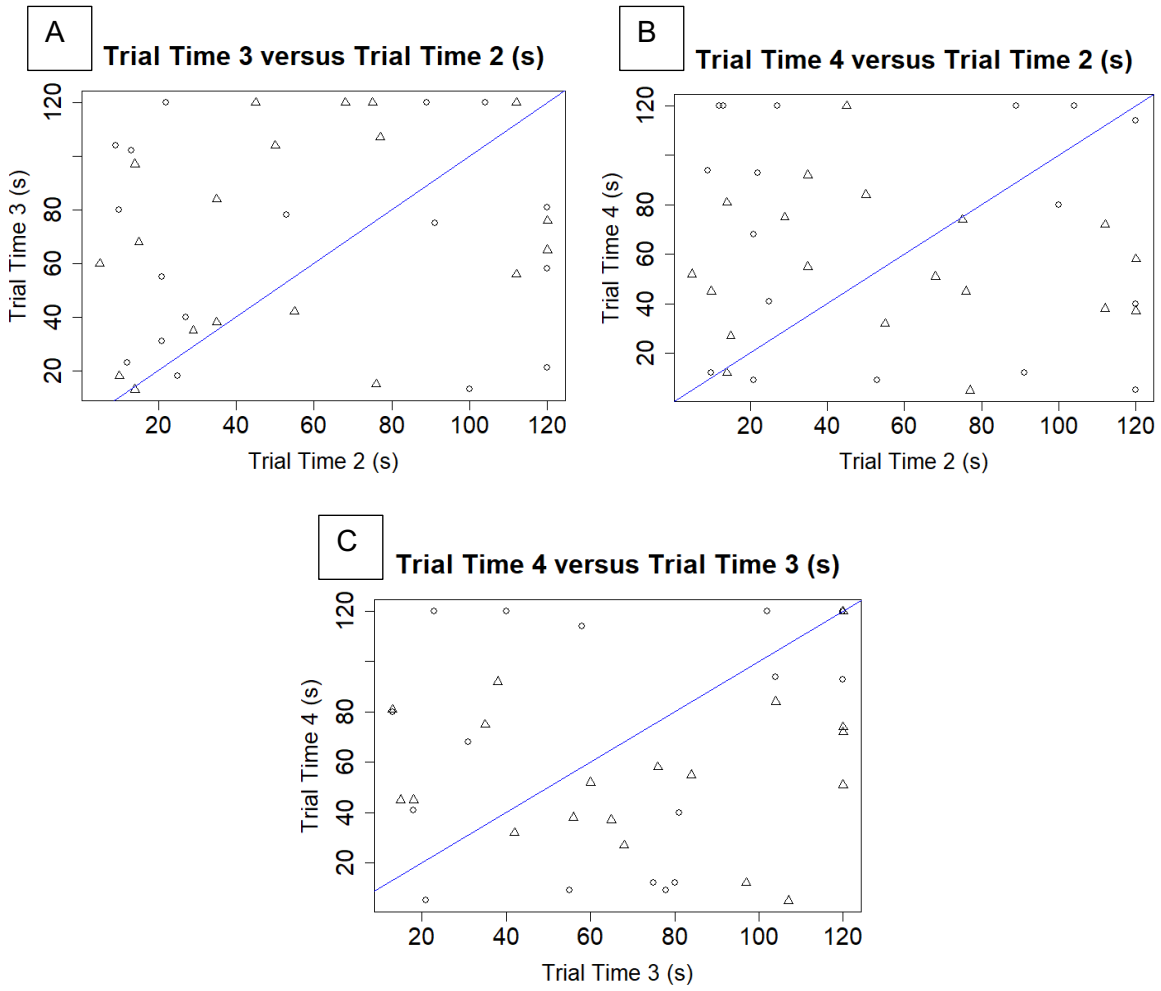

Figure 5. A. Boxmaze trial times 3 and 2 plotted against one another. **B.** Trial times 4 and 2 plotted against one another. **C.** Trial times 4 and 3 plotted against one another. Due to the absence of discernible natural clustering among mouse groupings, clustering analysis was ruled out as a way to represent the heterogeneity of cognitive impairment levels in mice assessed by the Boxmaze test. N=39.

Multiple linear regression can be used to estimate cognitive impairment effect of AAV-vectors on mice with different baseline cognition levels.

To examine the AD-related cognitive impairment development in the aging brain, the AAV-vector gene transfer method was chosen for the employment of the Aβ deposits and phosphorylated tau pathology distinctive in AD brains. This neuropathology background would

provide the appropriate setting to conduct tests that predict whether mice show differences in resistance to progressing cognitive decline (**Figure 6**). However, the preliminary step was to confirm that the vectors successfully reached influence on the behavioral level and indeed reduced cognitive function in mice. Multiple regression was chosen to provide this confirmation because the cognition assessing tests were screened at different timepoints, so the chosen response $'y'$ needed to relate to multiple covariate predictors simultaneously; it was necessary the analysis model system consider different potentially predictive variables of mice cognitive ability to calculate the actual cognitive change and ergo resistance to AD progression. First searching for any evidence that the AD vector was diminishing cognitive function more severely than the Sham vector, comparative linear regression coefficient analysis was done.

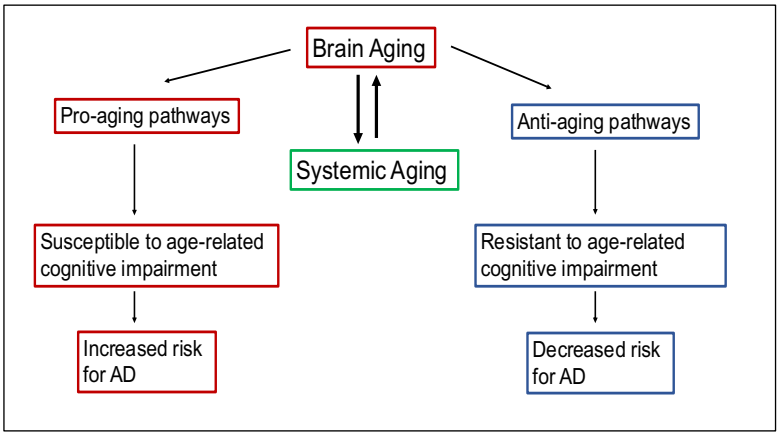

Figure 6. Brain aging and systemic aging factors contribute to age-related cognitive impairment and pathogenesis of Alzheimer's disease neuropathological features and dementia.

The response chosen was post-AAV Boxmaze performance and the predictors chosen were pre-AAV Boxmaze performance (baseline cognitive ability), and infected AAV-vector type (AD or Sham). In other words, the makeup of baseline cognitive ability and the effects of infected AAV-vector type would predict the post-AAV Boxmaze visuospatial cognitive ability. The linear model is the following:

$$E[y|x,T] = \beta_0 + \beta_1 x + \beta_2 T$$

In pre-AAV trials, Trial 1 marked the subject's first exposure to the maze and Trial 2 served as the acclimation phase, deeming both uninformative. The informative Trials 3 and 4 pre-AAV and all 4 trials post-AAV were weighed equally with x = average pre-AAV time in seconds of Trial 3 & 4. y = average post-AAV time in seconds of all 4 trials. Mice were administered AD vector or Sham vector indicated by T = 1 or 0 respectively. The βs are slope parameter coefficients determined by the sample data. The distribution assumption of post-AAV Boxmaze data was Gaussian about its conditional mean, meaning a linear combination exists of the independent covariates and that the distribution has the same variance throughout; the variance was not dependent on the covariates no matter what the values of the independent values were.

How effective the presence of AAV-AD-vector, T, is in changing y (post-AAV Boxmaze average), the measure of cognitive function after vector imposition, is determined by β_2. β_2 can be interpreted in this way: 2 mice with the same average pre-AAV time but where one was given the AD vector and the other was given the Sham vector, the conditional expectation of the AD-administered mouse is β_2 higher or lower in time post-AAV compared to the Sham-administered mouse. The value of β_2 tells the magnitude of the effect of AAV-vectors, and its sign tells the direction of the AAV-vector effect.

$$H_0: \beta_2 = 0$$
$$H_a: \beta_2 \neq 0$$

There is evidence of AAV-AD having a non-zero effect on Boxmaze performance by multivariate linear regression.

Graphically visualizing the difference between pre-AAV and post-AAV Boxmaze performance, 2 lines can be plotted in $y = \hat{\beta}_0 + \hat{\beta}_1 x + \hat{\beta}_2 T$ form, one each for $T = 1,\ T = 0$ (with AAV-AD or AAV-Sham), where the β in the population model have been replaced by their estimates (**Figure 7**). The difference between the two lines indicate the effect of AAV-vector distribution on

cognition. If a point is below the line $f(x) = x$, then the corresponding mouse had a faster average post-AAV trial time than average pre-AAV trial time. If a point is above, it was slower post-AAV.

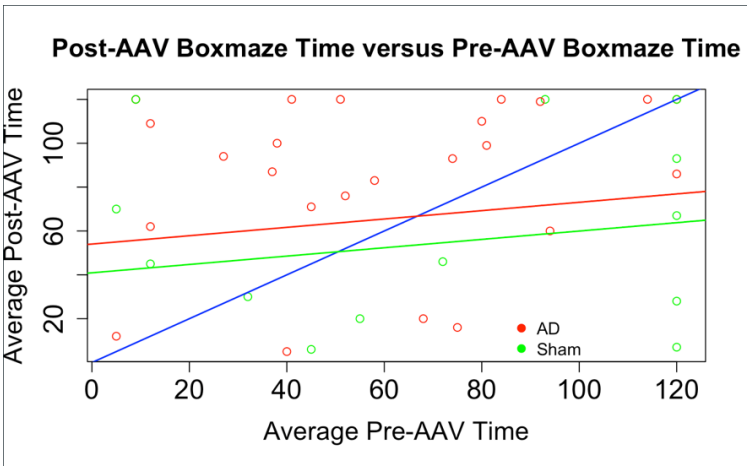

Figure 7. Multivariate linear regression for AAV-vector effects on Boxmaze performance in AD-administered and Sham-administered mice. N=14 for Sham, 25 for AD.

Table 2.

Estimate	Standard Error	p-value	95% Confidence Interval
$\widehat{\beta_2}$ = 10.96	7.88	0.17	(-4.48, 26.40)

Included in Table 2 is an approximate 95% confidence interval for $\widehat{\beta_2}$, which is computed as $(\widehat{\beta_2} - 1.96 \times Standard\ error \beta_2 + 1.96 \times Standard\ error)$.

Table 3.

Parameter Estimate	$\widehat{\beta_0}$	$\widehat{\beta_1}$	$\widehat{\beta_2}$
Value	42.18	0.18	10.96

The mice given AAV-AD slowed down in the post-AAV Boxmaze assay compared to those who received AAV-Sham. On average, the post-AAV performance of AD cohort mice was slower by roughly 11 seconds compared to the post-AAV performance of Sham cohort mice with the same average pre-AAV time. The p-value for the null hypothesis test that $\beta_2 = 0$ was 0.17, which is not below the standard statistical significance threshold of 0.05. Under the linear regression

model, the vector type did not have a non-zero effect on the Boxmaze performance of mice 2 months after their introduction. Although the test did not yield statistical significance, the AD mice cohort still displayed higher average post-AAV Boxmaze time than the Sham mice cohort.

Mice with better baseline spatial learning ability are not more resistant to cognitive impairment by multivariate multiple linear regression.

The next question posed to reveal whether resistance in cognitive impairment development is about the predictability of the degree of effect of the AD-vector operation by the initial pre-AAV cognitive ability of mice. For this, another linear model was used but an interaction term was added between AAV-vector type and pre-AAV average time.

$$E[y|x,T] = \beta_0 + \beta_1 x + \beta_2 T \ + \beta_3 Tx$$

In this model, the vector's effect varies based on the baseline pre-AAV performance (x), which can be rewritten $E[y|x,T] \ = \beta_0 + \beta_1 x + T(\beta_2 + \beta_3 x)$.

$$H_0: \beta_3 = 0$$
$$H_a: \beta_3 \neq 0$$

Here, if the effect of vector depended on the baseline measurement of cognitive function, for every increase of 1 second of average pre-AAV trial time, the effect of AAV-vector would either increase or decrease by β_3. **Figure 8** shows the regression model with the estimated coefficients in place of the β terms both with and without the $\beta_3 Tx$ term in question ($y = \hat{\beta}_0 + \hat{\beta}_1 x + \hat{\beta}_2 T \ + \hat{\beta}_3 Tx$ in red, and $y = \hat{\beta}_0 + \hat{\beta}_1 x + \hat{\beta}_2 T$ in green, where in both T is set to 1). The difference between the two lines illustrates how the effect of AAV-AD transduction in Boxmaze performance varies with x. The effect of AD-vector transduction's range can be calculated by varying x from 0 to 120 seconds and computing the estimates for the regression coefficients in the expression $(\beta_2 + \beta_3 x)$. Therefore, the effect of AD-vector transduction varied from 13.11 to 9.51 seconds. This range was positive throughout, confirming that the AD vector infliction

always indicated a larger average post-AAV Boxmaze performance when compared to the Boxmaze results of those same mice pre-AAV.

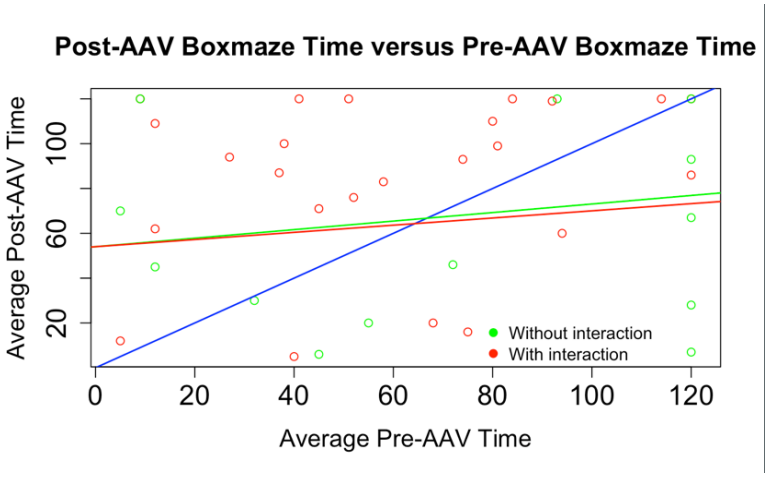

Figure 8. Multivariate multiple linear regression testing pre-AAV cognition levels interacting with function of AD-transfection on post-AAV Boxmaze performance. N=14 for Sham, 25 for AD.

Table 4.

Parameter Estimate	$\widehat{\beta_0}$	$\widehat{\beta_1}$	$\widehat{\beta_2}$	$\widehat{\beta_3}$
Value	40.9	0.19	13.11	-0.03

Table 5.

Estimate	Standard Error	p-value	95% Confidence interval
$\widehat{\beta_3} = -0.03$	.26	.91	(-.54, .48)

Included in Table 5 is an approximate 95% confidence interval for $\widehat{\beta_3}$, which is computed as $(\widehat{\beta_3} - 1.96 \times Standard\ error\beta_3 + 1.96 \times Standard\ error)$.

Because the estimate of β_3 is very close to zero, the sign is not important in interpretation. $\beta_3 = 0$ denotes that the effect of the AD vector infliction did not depend on x, the pre-AAV Boxmaze performance. The p-value of the test that $\beta_3 = 0$ is 0.91, which is well above the standard significance threshold of 0.05. Under the regression model, there is not enough evidence to reject the null hypothesis that the effect of AAV-vector depends on the baseline cognitive measure of average pre-AAV trial time. In other words, the potency of the AD vector's

biomechanistic virulence did not change depending on the baseline cognitive measure of average pre-AAV Boxmaze performance.

This model allows for the effect of vector transduction to depend on pre-AAV time, to investigate whether the variability in AD progression depends on baseline cognitive levels. It examines the interaction between pre-AAV Boxmaze performance averages and AAV-vector type. Though this linear interaction between pre-AAV Boxmaze cognition levels and AD or Sham introduction was not found to be statistically significant, there is room for uncertainty in making the same conclusion on a non-linear relationship between the two. However, there could be non-linear function of trial times that is different than the average Boxmaze measures which better captures the interaction between pre-AAV time and vector type. Average does not consider time component, which is essential to measuring learning in the philosophy of the Boxmaze.

In effect, the Boxmaze task aims to measure rate of learning over trials which looks at the improvement in performance rather than the average performance. As a result, there may exist a non-linear function of pre-treatment times which does have a relationship with post-treatment time. between the inputted covariates from raw average variables and regression. The variable of interest, $\hat{\beta}$ changes conditional to the sample pool. The sample variables of interest from this current selection of Boxmaze analysis-type is perhaps off-scale and unsuitable to accurately represent the effect the AD vector has on cognition in relation to learning reinforcement, in a linear fashion. Multiple linear regression may not better represent the true relationship of pre-AAV Boxmaze data and natural levels of cognitive impairment measured by visuospatial learning ability. Furthermore, what is needed is a different analysis method that accounts for all transformed Boxmaze learning data across sample cohorts in the experimental population and reconciles the challenges of analyzing composite data points separated by time.

Spatial Learning Index is developed as a criterion for scoring resistance to cognitive impairment.

Different baseline levels of cognitive functions are likely to significantly affect learning exemplified by Boxmaze performance. **Figures 1 & 2** show fluctuations that represent the varying patterns in average Boxmaze performance and inter-trial change distribution, illustrating some mice develop an accurate search strategy or have better learned recall ability than others. So to represent the variation in susceptibility or resistance to cognitive decline associated with age, a ranking system using composite scores that consider the rate at which learning is acquired may be effective.

Simply relaying and connecting shorter latency observance to faster learning and higher levels of cognition is an imprecise equivalence which highlights the importance of a new measure to characterize individual differences on the effects of aging on task learning strategy. Therefore, the spatial learning index developed for MWM was adapted here into a more robust mathematical system to provide a graded measure of place learning acquisition via the Boxmaze assay. This method can show whether mice display heterogeneity in resistance to naturally induced aged cognitive impairment.

The learning index was developed in the following way. Pre-AAV Boxmaze trial times from trials 2, 3, and 4, called, '$\boldsymbol{b}$', '$\boldsymbol{c}$', and '$\boldsymbol{d}$' respectively, were each compared to the timestamp of trial 1, called '$\boldsymbol{a}$', to calculate the degree of improvement with respect to the first trial. Considering 1 is the greatest possible score for holistic improvement, each of the 3 ratios (formed from $\boldsymbol{b}$, $\boldsymbol{c}$, and $\boldsymbol{d}$) was subtracted from 1 to represent the degree of improvement within one of the last 3 trials, compared against the first trial, for a single mouse (ex: $1 - (b/a) = (a - b)/a$). Empirically, due to the pronounced drops in time from Trial 1 to Trial 2, which signals greatest learned

acquisition, the dataset generally saw that the ratio from Trial 2 had the strongest influence in learning index composition (**Table 8**).

Given that there was a relatively large range and spread of numbers in the distribution of average trial times of the entire pre-AAV Boxmaze dataset, in between each mouse experiment as well as whole trial averages, and because the extent of place learning that took place after each time of exposure held different improvement significance, there was a need to weigh trial times such that they rewarded consistently improving rates of place learning over trials and penalized slow rates of place learning after the first exposure. The weighted system would normalize the dataset to one more accurately representative of the population-wide, if not, the sample-wide spread of baseline (pre-AAV) cognition levels. This allowed the amplification of the learning index spectrum, which let smaller changes in individual learning improvement levels be scaled into accountable measures.

The statistical variances per the 4 trial times contributed to the formation of the weighted multipliers, which were derived directly from the quotients of each one of Trial 2,3, or 4 dataset's variance and Trial 1 dataset's variance. To add power, the variances were derived from a sample dataset of Boxmaze data of 20 male and 20 female 24-month old C57BL/6 mice from a collaborative bioarchive database in the Ladiges Lab, in addition to this current project's assembly of 39 mice. The variance calculation results are shown in **Table 6**.

Table 6. Composite baseline Boxmaze trial variances determined by for all mice in study + bioarchived Boxmaze data sample of 20 male and 20 female 24-month old C57BL/6 mice

Composite Trial 1 Variance	**Composite Trial 2 Variance**	**Composite Trial 3 Variance**	**Composite Trial 4 Variance**
823.333	1666.166	1676.163	1886.371

Trial 1 variance was treated as the point of standard variance in learning improvement to create the multiplier series because mice were first introduced to the Boxmaze in Trial 1, which resulted in multiplier ratios calculated with respect to Trial 1. The multiplier calculation results are shown in **Table 7**. The first trial time, which is usually a relatively higher number, was necessary only as the starting reference performance. Consequently, the first trial's multiplier is always going to be 1, so it was not included in the multiplier series.

The multiplier series shows that the greatest variance in performance in the last trial would be weighed the heaviest since largest variance means the most heterogeneity of scores within the trial-specific dataset, and observance of the capacity of mice to learn. The underlying presumption is that mice at opposing spectrum of cognitive function will display their learning ability divergence the most after more exposures to the maze. The little variance in performance in the second trial would be weighed the lightest since least variance means the smallest frame of confident learning improvement consistency of the scores from that trial. The improvement calculating numerals (**Table 8**) were multiplied by the multiplier series respective to trial number, omitting the first trial's product. The rest of the 3 products were summed to form the spatial learning index score.

In short, the learning index was made up in the following steps for one mouse: Find the variance values per all 4 trials from all mice that underwent Boxmaze. The variance values will make up the multipliers that will be used to weigh each trial differently. To come up with the multiplier series, use the variance from Trial 1 as the denominator and the variance for the remaining trial numbers as the numerators for each respective trial. Exclude the product of the first multiplier number (variance of Trial 1/variance of Trial1) in the later calculations. The multiplier series will be the 3 ratios in order. Take the performance of each of Trials 2,3,4 and divide with the timestamp of Trial 1. Subtract each of the 3 quotients from 1 so there are 3 numbers left (mostly

irrational decimals) for each mouse $(ex: 1 - (b/a) = (a-b)/a)$. These are the raw improvement scores. Find the multiplicative product of the multiplier series and the raw improvement scores, save the first trial. Add up the 3 calculated scores from Trials 2,3,4 belonging to each mouse to form the learning index.

For a statistical description: given a set of 4 elements, each element assigned a multiplier weight and a numerical measure based on Boxmaze trial time performance, sum the product across the elements (from $i = 2$ to $i = 4$), to find a solution such that the weighted sum of squares contributes to the overall Boxmaze Learning index.

$$Boxmaze\ Learning\ Index = \sum_{i=2}^{4} (Mi \times Si)$$

Table 7. Multiplier series made up of ratios of variances of Boxmaze trial averages

M1	M2	M3	M4
1	0.599	0.579	0.645

Table 8. Improvement scores made up of differences of ratios of individual trial times

S_1	S_2	S_3	S_4
$1 - (\frac{a}{a})$	$1 - (\frac{b}{a})$	$1 - (\frac{c}{a})$	$1 - (\frac{d}{a})$

a, b, c, d refer to the raw time performance for a mouse for trials 1, 2, 3, 4 respectively.

Learning index scores discriminate differences in Boxmaze performance. In theory, the entire population of mice would span a spectrum where at one end, there would be mice that display the worst learning capability and on the other end, there would be mice that have optimal possible learning capability. The learning index display differences in cognitive function namely learned visuospatial navigation and is useful to correspond and match mice to similar levels of cognitive impairment.

Post-AAV Boxmaze trials were considered a continuation of the pre-AAV Boxmaze data long term memory measurements (**Darvas et al., 2019**). Post-AAV Boxmaze Trial 1, Trial 2, Trial 3, and Trial 4, relabeled 'e','f','g','h' respectively, were each divided by pre-AAV Boxmaze a to account for the fact that mice were already assimilated to the learning space environment and could implement their long term memory ability to complete the assignment. The post-AAV learning index was calculated and compared with the pre-AAV learning index to observe the scope of changes in scores across vector type groups.

Boxmaze spatial learning index correctly differentiates AAV-vector types.

To ensure that the learning index scoring system truly reflects learning in Boxmaze and that the effects of the different vector administration are robust enough to present through Boxmaze performance, the post-AAV learning index scores were tested for their ability to discriminate between Sham or AD vector inducement using a ROC curve and AUC score. If mice given the AD vector had distinctly lower post-AAV learning indexes than their Sham vector counterparts, the sensitivity and specificity of the learning index scoring system should convey the ability to correctly identify mice with the cognition-compromising condition and mice without. Here, the AUC score quantifies the overall discriminative ability of the post-AAV learning index for the 2 vector conditions. It is taken from the ROC curve, a graphical representation of the tradeoff between sensitivity and specificity at various thresholds for a binary predictor model. Sensitivity, or the true positive rate, tells the proportion of actual positives correctly identified by the model. The greater the sensitivity, the lower the likelihood of the model yielding false negatives, which are instances where the post-AAV learning index fails to detect AD mice. Specificity, or the true negative rate, measures the proportion of actual negatives that the learning index model correctly recognizes. A test with greater specificity produces fewer false positives, which occur when the post-AAV learning index incorrectly indicates an AD mouse. With TPR (sensitivity) on the y-axis and FPR (1-specificity) on the x-axis, shown in **Figure 9**, an AUC of 0.7 indicated the

post-AAV learning index is generally a good predictor and can distinguish the vector type-induced cognitive learning differences; the learning index model is able to detect more numbers of true positives and true negatives than false negatives and false positives. The red line $y = x$ shows an instance of when an AUC = 0.5, which suggests no discriminative ability and the learning index scoring system is no different to random guessing at distinguishing between AD and Sham groups. The ROC curve analysis, with an AUC of 0.7, suggested that the post-AAV learning index effectively differentiates between the AD and Sham control groups. This implied that the 2 cohorts exhibit distinguishable Boxmaze performance variations, validating the learning index as a reliable metric for analyzing cognitive impairment levels.

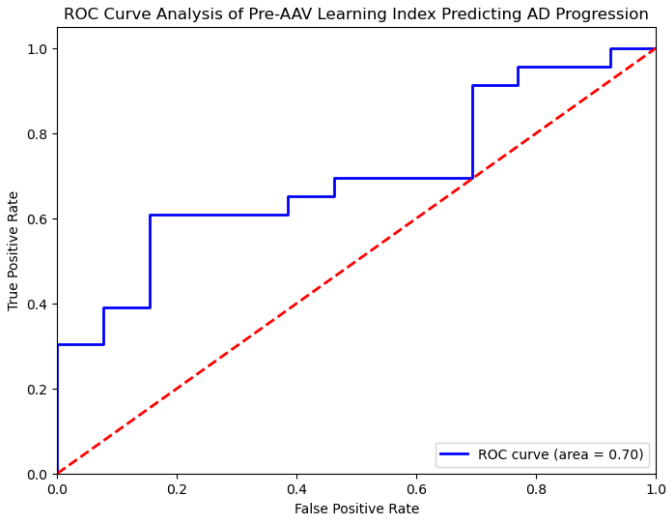

Figure 9. Receiver Operating Characteristic (ROC) curve illustrating discriminative performance of the post-AAV learning index in identifying between the AD and Sham groups. An Area Under the Curve (AUC) of 0.7 indicates a good level of accuracy in the learning index ability to classify the cognitive impairment status of the mice based on their Boxmaze performance. N=39.

Pre-AAV Boxmaze spatial learning index distinguishes resistance to cognitive impairment in post-AAV Boxmaze test.

In order to run statistical analyses using the learning index scale, the underlying distribution of the variable was investigated. Bootstrapping is a resampling method to estimate the distribution of a statistic by sampling with replacement from the original data, allowing for the approximation of the sampling distribution. Used where the form of theoretical sampling distribution is unknown

or difficult to derive analytically and with small sample sizes, it relies on the law on large numbers, where characteristics of a sample approximate the corresponding characteristics of the larger population it was drawn from. In this case, the pre-AAV learning indexes were repeatedly resampled from the sample pool and a bootstrap distribution was generated (**Figure 10**).

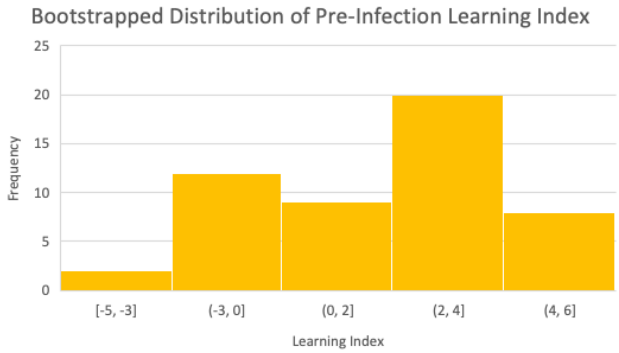

Figure 10. Bootstrapped distribution of pre-AAV learning index scores. Pre-infection = pre-AAV.

The bootstrapped Boxmaze learning index distribution showed a skewed histogram, denoting the population of learning index is not normally distributed. Shapiro Wilk test and subsequent QQ plot graphing was used for regression normality testing. Both showed evidence of non-Gaussian distribution. Comparing the quantiles of the learning index dataset to the theoretical quantiles of the normal distribution, QQ plot data point alignment along the reference line of theoretical ratio 1, was visually assessed, where the dataset showed a skewed curvature (**Figure 11B**). Because neither the Shapiro-Wilk test **(Table 9)** nor the QQ plot showed evidence of a normal distribution, the analyses involving the learning index were for non-Gaussian assumed variable distribution.

Table 9. Shapiro-Wilk test of Pre-AAV Learning Index, Post-AAV Learning index data

Shapiro-Wilk test	Pre-AAV Learning Index	Post-AAV Learning Index
W	0.7066	0.9168
P value	<0.0001	0.0089
Passed normality test (alpha=0.05)?	No	No
P value summary	****	**

There were differences in average learning index in comparisons of both vector type and sex. The post-AAV learning index results were more condensed and showed descending trends from the pre-AAV learning index spread, broadly showing that after 2 months of either vector regiment, mice visuospatial learning cognitive levels fell as expected by cohort (**Figure 11A & B**). However, looking at groups within the post-AAV learning index (**Figure 11D**), despite the cognition debilitating vector infliction, female AD mice showed stronger resiliency to cognitive decline, having higher average post-AAV learning index levels than the female Sham mice (p=0.125) (**Supplementary Table 3**). Still, in the males, the AD group ceded lower post-AAV performance than the Sham group (p=0.367, **Supplementary Table 4**), though in both cases the differences were not significant by the Mann-Whitney test. **In Figure 11F**, the post-AAV learning index linear regression slope of Sham mice is bigger than that of AD mice. Generally speaking based on these trendlines, if an AD and Sham mouse had the same learning index score before vector introduction, the AD mouse had lower learning index than the Sham mouse post-AAV, confirming the index evaluates Boxmaze performance as expected according to cohort. But there was no significant difference comparing the slopes of AD or Sham groups on post-AAV learning index by two-tailed T-test (t(32)=0.9688, p=0.3399, **Table 10**).

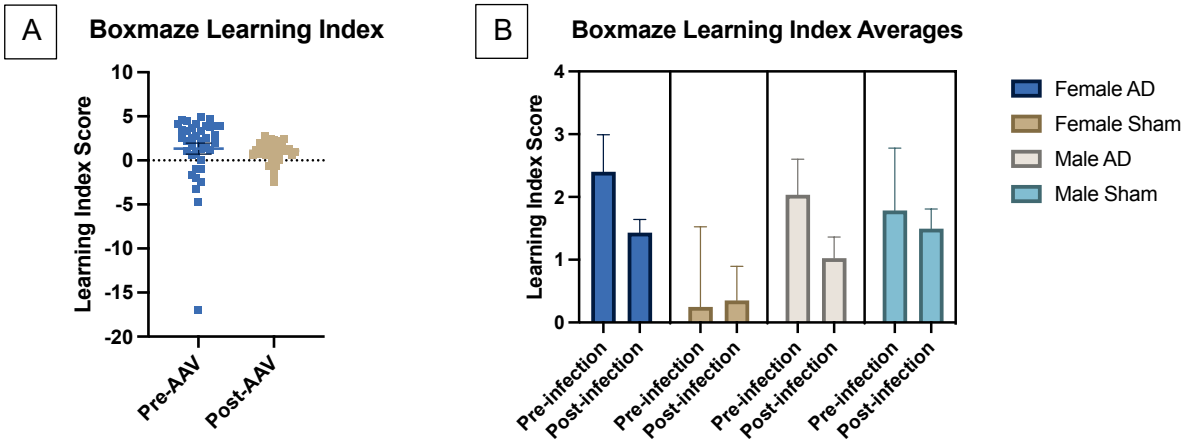

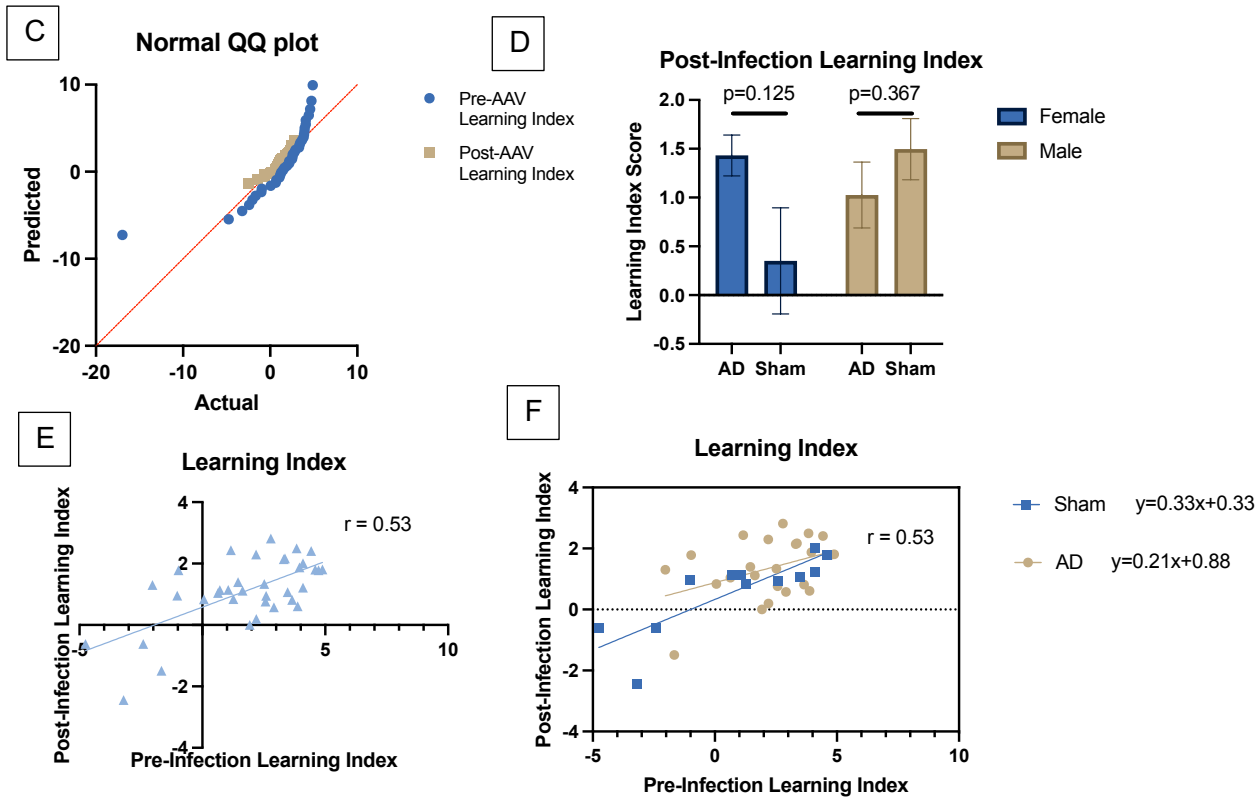

Figure 11. A. Scatter distribution of Pre-AAV Learning Index and Post-AAV Learning Index. **B.** Bar chart showing pre-AAV and post-AAV learning index averages per sex and vector cohort. **C.** QQ Plot of Pre-AAV Learning Index and Post-AAV Learning Index. **D.** Post-AAV learning index by vector type and sex cohorts, analyzed for significance by the Mann-Whitney test. **E.** Linear correlation analysis between pre- and post-AAV learning index regardless of vector type (Spearman correlation r=0.53) confirms learning index scores evaluate Boxmaze performance at large. **F.** Scatter plot showing linear correlation between pre-AAV and post-AAV learning index (Spearman correlation r = 0.53). Significance is set at p<0.05 and is indicated by *. N = 5-14 per cohort.

Table 10.

$Slope_{AD}$	$Slope_{Sham}$	$Standard\ Error_{(difference)}$	p-value	T estimate
$\widehat{\beta_0} = 0.21$	$\widehat{\beta_0} = 0.33$	0.12	0.34	0.97

Dealing with matched subjects in pre- and post-AAV Boxmaze learning indices, Wilcoxon matched-paired signed-rank test (scatter plot shown in **Figure 11F**) assessing for a change in the learning index following vector inoculation showed a strong but not statistically significant difference in the average sums of ranks and medians between two data of the two timepoints (p=0.0884) (**Supplementary Table 5**). Overlaying the related pairs of learning indices pre- and post-AAV without distinguishing vector type, the Spearman correlation coefficient, r= 0.5311, showed moderate positive correlation between the variables. Pre-AAV learning index was able

to predict post-AAV learning index in a consistent manner (significant effective pairings p=0.0004, one tailed) **(Supplementary Figure 5).**

Pre-AAV learning index may predict other brain aging parameters.

Under the geroscience paradigm, aging and related cognitive impairment processes occur via multiple pathways in different individuals at different speeds **(Ladiges and Liggitt, 2018).** If the Boxmaze learning index extends as a metric for cognition, can it be correlated with future cognitive impairment phenotypes? Can evaluating the correlation predict other aging related parameters and foretell further memory impairment? Can resilience to cognitive impairment be measured early in the process? White blood cell counts, the Y-maze behavioral assay, and IHC were compared to investigate these ideas.

White blood cell measurements are not predicted by pre-AAV learning index.

Cognition is impaired by chronic exposure to stressors and pathogens that can also result in immuno-physiological responses **(Benros et al., 2015)**. In an attempt to replicate the correlation between immune response and cognition, WBC counting experiments were conducted. Increased glucocorticoid responses and immunosuppression, indicating the body's ability to fight infections and other immune system functions, are examples of these physiological responses **(Hickman, 2017)**. These changes can be measured by looking at neutrophil to lymphocyte ratios (NLR), a reflection of the balance between the body's immediate and long-term defense mechanisms against stress. NLR is also a marker showing systemic inflammation and stress levels in relation to cognitive decline and neuropathology, such as AD **(Zenaro et al., 2015)**. Neutrophilia, an increase in the number of neutrophils, or lymphopenia, a decrease in the number of lymphocytes in the blood, demonstrate the aftermath of actions by the first line of defense or adaptive immunity observable in chronic illnesses. Chronic pathogen exposure can lead to persistent immune system activation which in turn can impact cognitive function. Total

WBC counts and NLR were measured to infer levels of stress and link them to cognitive impairment.

Generally, females had lower post-AAV total WBC counts whereas males had higher post-AAV total WBC counts than their respective pre-AAV counterparts. Males consistently had higher total WBC counts and NLR ratio averages than females, but there were no other consistent correspondences according to pre-AAV and post-AAV measurements (**Figure 12A, B, C, E**).

3-way ANOVA was chosen to determine the numerical relationship between 3 variables on WBC data and their related source of variation, whether the effect of one factor depended on the level of another factor (**Supplementary Table 6 & 8).** Looking at the variability main effects between the combinations of cohorts, there was a significant effect between female and male groups in the total WBC count ($F[1,29]=10.65$, $p=0.0028$) and NLR ($F[1,34]=11.88$, $p=0.0015$). The time effect (pre-AAV vs. post-AAV) did not show a statistically significant main effect on the total WBC count ($F[1,29]=0.4096$, $p=0.5272$) nor on the NLRs ($F[1,34]=0.2640$, $p=0.6107$), which follows then that the AAV-vector (AD vs. Sham) did not show a significant main effect in WBC counts ($F[1,29]=2.814$, $p=0.1042$) nor NLR ($F[1,34]=0.1098$, $p=0.7424$). For both WBC and NLR measures, the interaction effects of the interaction between sex and time effect, sex and vector type, and time effect and vector type were not statistically significant (WBC: $p=0.0438$, 0.9214, 0.6157; NLR: $p=0.1629$, 0.7565, 0.9306), except for WBC's interaction between sex and time effect ($F[1,29]=4.444$, $p=0.0438$).

After fitting a 3-way ANOVA model accounting for interactions of sex, vector type, and time effect, in both total WBC counts and NLR measures, post-hoc Sidak's multiple comparisons test was conducted to assess all possible pairwise mean differences and look for the source of variation (**Supplementary Table 7 & 9**, for summary of pairwise comparisons). For total WBC

counts, significant mean differences were observed between ‘Female: AD Post-AAV’ and ‘Male: AD Post-AAV’ (Predicted LS mean difference=-18492), 95% CI of difference [-33679, -3305], Sidak-adjusted p=0.0074) (**Figure 12D**). No other significant differences were found comparing all the other group pairs in the multiple comparisons test (**Figure 12F**). These results suggest that sex difference may play a significant role in the post-AAV immune function outcomes for AD mice cohorts, with male mice exhibiting a statistically different response in elevated WBC counts compared to their female counterparts under similar post-AAV-AD conditions.

Regardless of vector type, the correlation analysis with the WBC total counts or NLR and learning index did not show strong evidence of correlations (Spearman coefficient total WBC, NLR: r=-0.1697, r=0.3042) (**Figure 12G & H**). However, looking at the sectioning by vector type for WBC counts, the AD cohort had a steeper negative slope than the Sham cohort, meaning the mice of same cognition levels pre-AAV had lower total WBC count averages post-AAV with AD than with Sham, exhibiting that mice with AD are associated with decreased total WBC counts. But there was no significant difference comparing the slopes of AD or Sham groups on total WBC counts by two-tailed T-test (t(33)= 0.2878, p=0.7752) (**Table 11**).
Looking at the NLR averages, though there was no correlation with pre-AAV learning index, the AD mice had a much higher positive slope than the Sham mice (**Figure 12H**), showing mice with initially same cognition levels will develop increased NLR associated with pro-inflammatory state or increased stress if they were AD inoculated. But there was no significant difference comparing the slopes of AD or Sham groups on NLR by two-tailed T-test (t(33)= 1.214, p=0.2332) (**Table 11**).

Total WBC counts and NLR data showed that exposure to pathogenic effects of the AD and Sham vectors did not robustly act as a measure of cognitive impairment in mice. Since the NLR differences corresponded with a behavioral variable of stress in rats **(Hickman et al., 2014),** the

aim was to correlate learning index with the physiological outcome of WBC counts due to chronic inoculation by AD and Sham vectors, which parallels cognitive impairment. However, the interactions are muddled by the shortcomings of the data collection step's inability to extract analysis from nonsensical measurements.

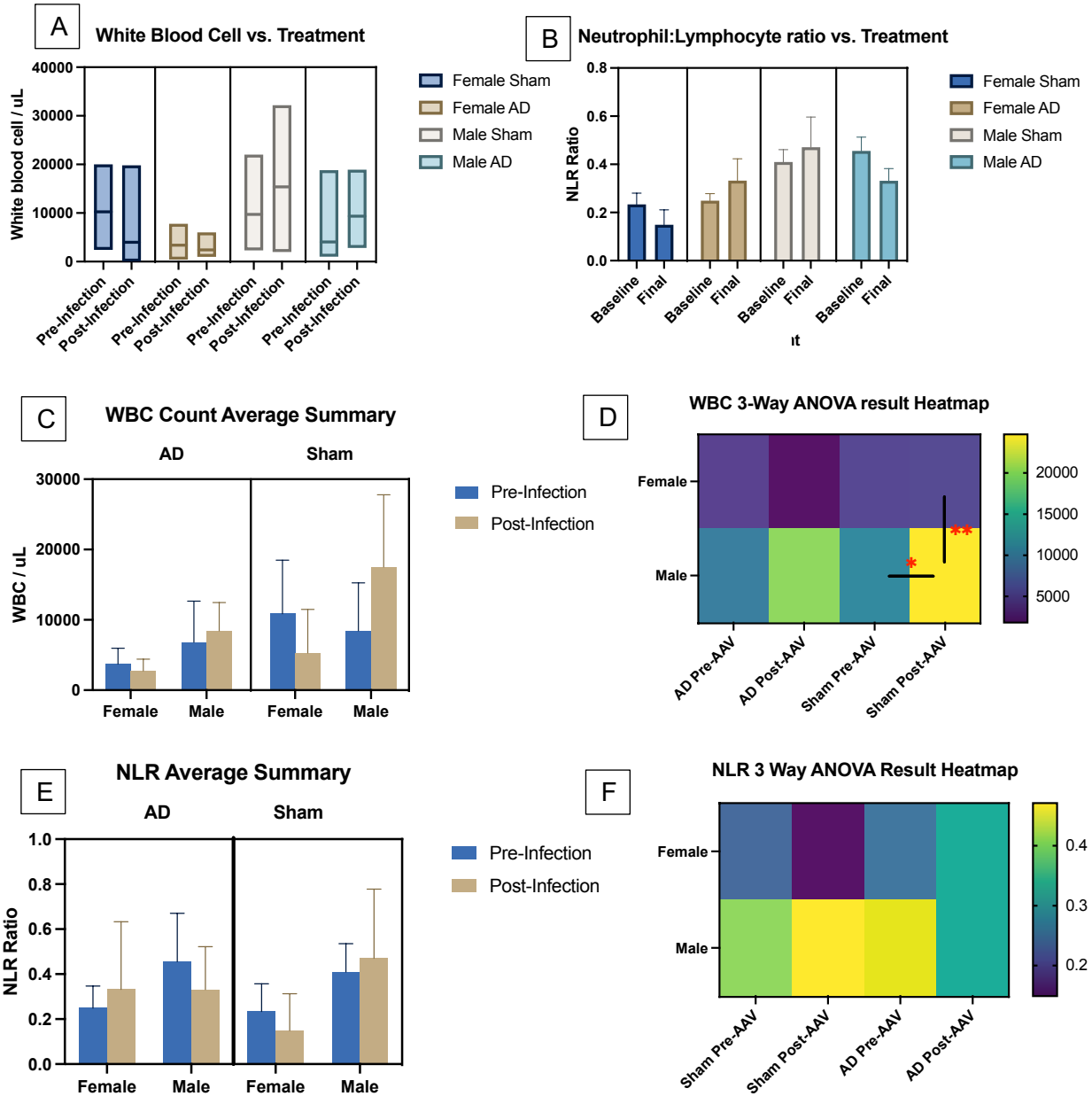

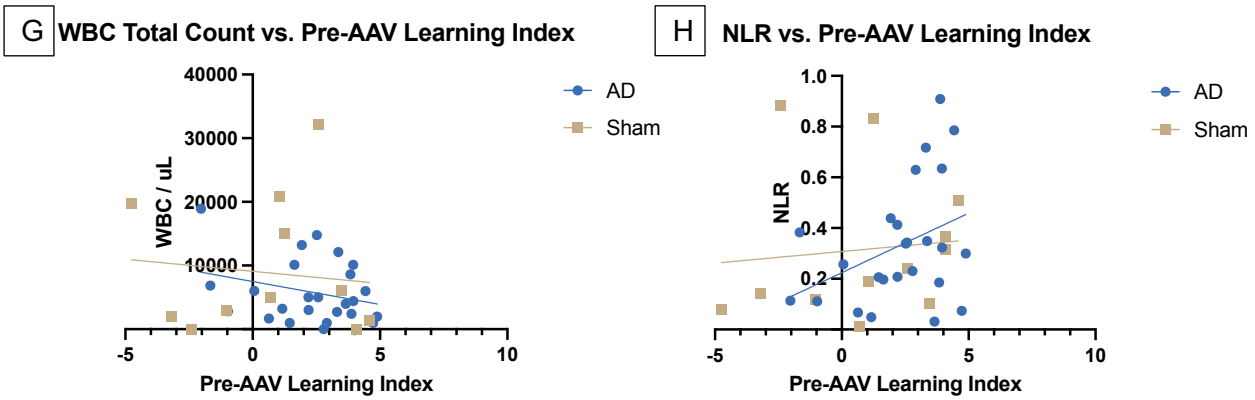

Figure 12. A. Low-high plot depicting total white blood cell counts/uL with middle line representing median, for all cohorts (Pre-infection – Pre-AAV, Post-infection – Post-AAV). **B.** NLR distributions for all cohorts (Baseline – Pre-AAV, Final – Post-AAV). **C.** Bar graph of WBC counts for all cohorts. **D**. Heatmap of WBC counts 3-Way ANOVA by cohort. **E.** Bar graph of NLR averages by cohorts. **F.** Heatmap of NLR 3-Way ANOVA results by cohort. **G.** Correlation analysis of WBC count by vector type. **H.** Correlation analysis of NLR by vector type. Significance is set at $p<0.05$ and is indicated by *. N = 5-14 per cohort.

Table 11.

$Slope_{AD}$	$Slope_{Sham}$	$Standard\ Error_{(difference)}$	p-value	T estimate
WBC $\widehat{\beta_0} = -721.7$	WBC $\widehat{\beta_0} = -380$	1187	0.33	0.29
NLR $\widehat{\beta_0} = 0.0469$	NLR $\widehat{\beta_0} = 0.0009$	1.214	0.23	1.21

There was no significant change in female and male body weight.

A 2-tailed unpaired T-test was performed to compare the means of Female AD and Sham weekly weights ($t(15) = 1.511$, $p=0.1517$), and the means of Male AD and Sham weekly weights ($t(18) = 0.9932$, $p=0.3338$). There was no significant change in weight over 9 weeks for female or male mice (**Figure 13**).

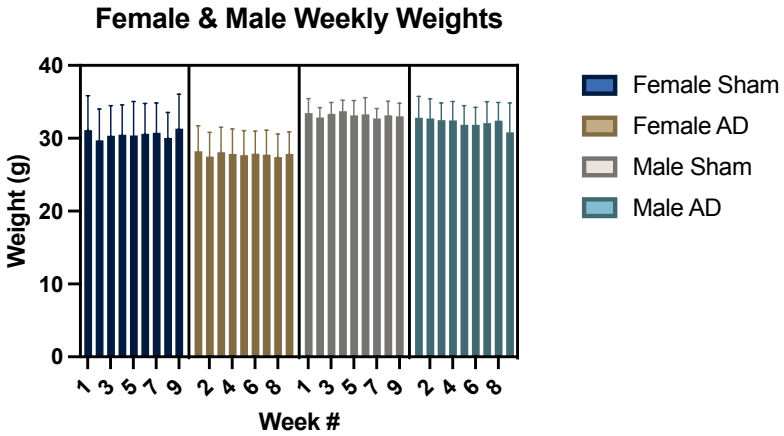

Figure 13. Bar plot showing mice weights over 9 week period. N = 5-14 per cohort.

Pre-AAV Boxmaze spatial learning index did not distinguish resistance to cognitive impairment by Y-maze assessment.

The Y-maze studies spatial learning and short-term memory and willingness to explore new environments. The test is on the ability to visit the arms of the maze at even rates, with calculated spontaneous alteration scores closer to 1 signaling more symmetry of the exploration into each of the arms of the maze, and indicating prime cognitive function. The Y-maze was conducted post-AAV after 2 months of viral amplification. Female Sham mice had slightly higher Y-maze spontaneous alteration ratio averages than Female AD mice. But surprisingly, male Sham mice had lower Y-maze spontaneous alteration ratios than the male AD mice (**Figure 14A)**. In assessing the responses of 4 mice cohorts across the 2 conditional variables (vector type and sex) within the Y-maze test, Krustal-Wallis H test failed to show significant differences in the central tendencies of the spontaneous alteration scores, with a Krustal-Wallis H value of 0.7635, p=0.8582, leading to the conclusion that the variations in spontaneous alteration scores are due to chance rather than the effects of vector type and sex delineated groups. For the Y-maze arm entry attempt numbers, the Kustal-Wallis H value was 11.83, p=0.008. Here, using Dunn's post-hoc multiple comparisons test, the only pair with significance was Female Sham vs. Male Sham with an adjusted p=0.0262 **(Figure 14B)**, leading to the conclusion that there was a sex difference in entry attempts in mice with normal aging background.

Using Spearman correlation on vector type and sex-pooled data, Y-maze spontaneous alteration ratios and pre-AAV learning index did not show statistically significant correlation, Spearman r=0.07158, 95% CI [-0.2725, 0.3994], p=0.6782 (**Figure 14C**). Similarly, learning index could not predict short term memory measure on Y-maze performance using the learning index by Spearman correlation, r=0.1061, 95% [-0.2351, 0.4240], p=0.5320 (**Figure 14D**).

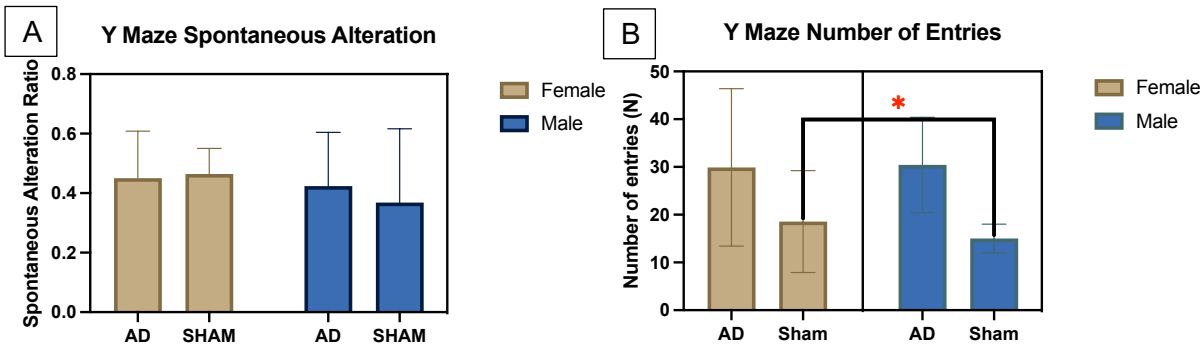
A
Y Maze Spontaneous Alteration
Spontaneous Alteration Ratio
0.8
0.6
0.4
0.2
0.0
AD
SHAM
AD
SHAM
Female
Male
B
Y Maze Number of Entries
Number of entries (N)
50
40
30
20
10
0
*
AD
Sham
AD
Sham
Female
Male

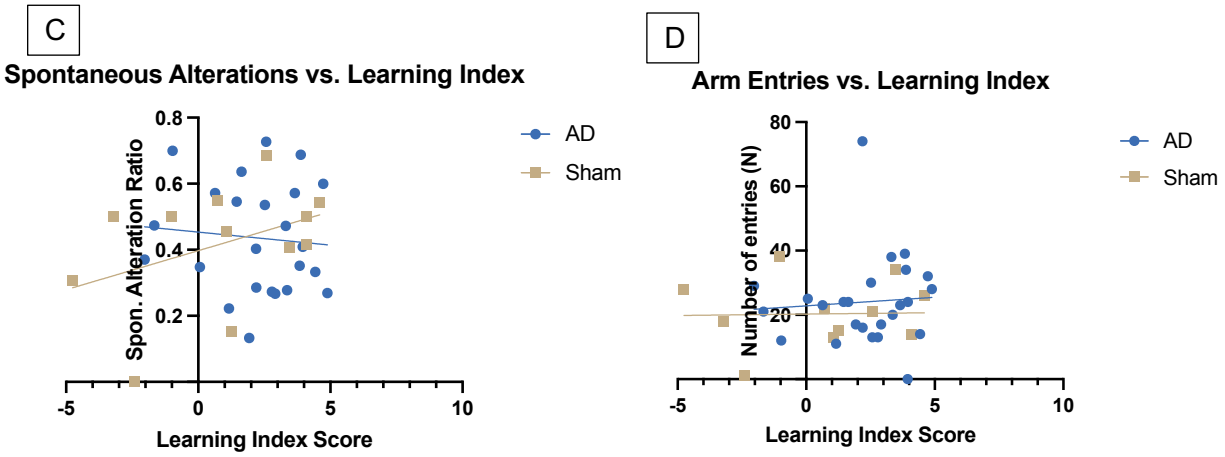
C
Spontaneous Alterations vs. Learning Index
Spon. Alteration Ratio
0.8
0.6
0.4
0.2
-5
0
5
10
Learning Index Score
AD
Sham
D
Arm Entries vs. Learning Index
Number of entries (N)
80
60
40
20
-5
0
5
10
Learning Index Score
AD
Sham

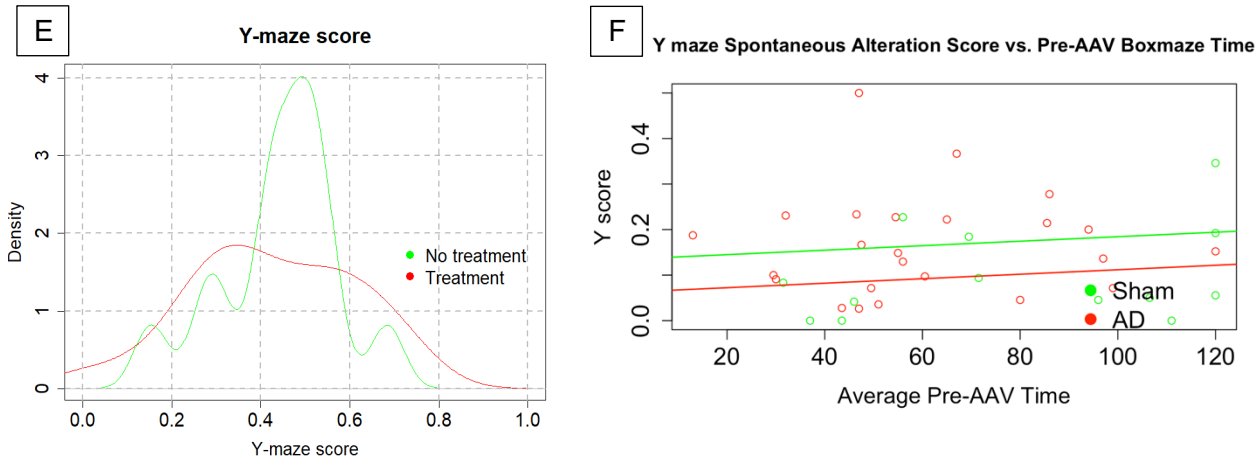
E
Y-maze score
Density
4
3
2
1
0
0.0
0.2
0.4
0.6
0.8
1.0
Y-maze score
No treatment
Treatment
F
Y maze Spontaneous Alteration Score vs. Pre-AAV Boxmaze Time
Y score
0.4
0.2
0.0
20
40
60
80
100
120
Average Pre-AAV Time
Sham
AD

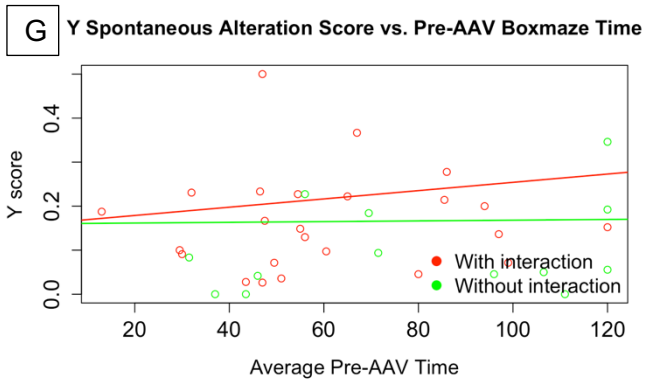

Figure 14. A. Distribution of Y-maze spontaneous alteration ratios by cohort. **B.** Distribution of number of arm entries in Y-maze by cohort. Krustal Wallis-H test with post-hoc Dunn's multiple comparisons test showed significant interaction between Female Sham & Male Sham groups, p=0.0262. **C.** Correlation analysis between pre-AAV learning index and spontaneous alterations, Spearman r = 0.07158. **D.** Correlation analysis between pre-AAV learning index and Y-maze arm entries, r= 0.08904. **E.** Kernel density estimate plot of Y-Maze data for AD and Sham vector administered mice, colored by vector type (No treatment - Sham, Treatment – AD). **F.** Multivariate multiple linear regression testing pre-AAV cognition levels on Y-maze spontaneous alteration scores, colored by vector type (Green - Sham, Red – AD). **G.** Multivariate multiple linear regression testing pre-AAV cognition levels interacting with function of AD-transfection on Y-maze spontaneous alteration performance, colored by vector type (Red points – AD, Green points – Sham, Red line – Model including interaction term, Green line – Model not including interaction term). Significance is set at p<0.05 and is indicated by *. N = 5-14 per cohort.

The kernel density estimate graph showed density of Y-maze score was more concentrated around 0.5 for Sham mice and was more uniformly spread out for AD mice. The average score for AD mice was 0.42 with a standard deviation of 0.19, while the average score for Sham mice was 0.44 with a standard deviation of 0.14 (**Figure 13E)**. The median of the AD group was 0.406 and the median of the Sham group was 0.454. Y-maze measures short-term cognitive function, and is another way to show cognitive health.

There was no significant evidence of AD-transduction having a non-zero effect on Y-maze performance.

Since Y-maze spontaneous alterations measurements are not raw data, but are processed data of the pattern of arm entrance attempts in organized sequence, it made sense to run parametric type statistical tests. Variance contributions from independent variables such as vector type and pre-AAV Boxmaze performance were observed for multivariate linear regression relation with Y-maze performance (**Figure 14F**). In the linear model: $E[y|x,T] = \beta_0 + \beta_1 x + \beta_2 T$, the Y-maze

score is an indicator variable of vector type (T= 0 or 1, AAV-Sham or AAV-AD), covariate x is the average pre-AAV time of Trial 3 and Trial 4 Boxmaze in seconds, y is the Y-maze spontaneous alteration score, and β terms are coefficients estimated through linear regression.

Table 10.

Parameter Estimate	$\widehat{\beta_0}$	$\widehat{\beta_1}$	$\widehat{\beta_2}$
Value	$.486$	-0.001	-0.027

Table 11.

Estimate	Standard Error	p-value	95% Confidence interval
$\widehat{\beta_2}$ = -0.027	0.062	0.67	(-0.149,0.096)

Included in Table 11 is an approximate 95% confidence interval for $\widehat{\beta_2}$, which is computed as $(\widehat{\beta_2} - 1.96 \times Standard\ error\beta_2 + 1.96 \times Standard\ error)$.

The conditional expectation of the Y-maze score of AD mice, is $\widehat{\beta_2} = 0.027$ lower than untreated Sham mice with the same average pre-AAV time (**Figure 13F**), which matches the expectation that AD should lower the cognition function. The p-value of the test that β_2 = 0 is 0.67; there was not enough evidence from the sample to reject the null hypothesis. Therefore, under the regression model, AAV-AD operation does not have a non-zero effect on Y-maze score.

Mice with better baseline spatial learning ability were not more resistant to cognitive impairment. The effect of AAV-AD vector did not depend on the pre-AAV cognitive ability of the mice.

Given stronger Y-maze performance relates to the untreated Sham vector transduction, perhaps the progression of cognition impairment by Y-maze results is best predicted by pre-AAV Boxmaze-measured cognition levels. For this, an interaction term is included as expressed in the linear model $E[y|x,T] = \beta_0 + \beta_1 x + \beta_2 T + \boldsymbol{\beta_3 T x}$. **Figure 14G** shows the regression lines of

the estimated coefficients (β terms) both with and without (red and green lines) the $\beta_3 Tx$ term ($y = \hat{\beta}_0 + \hat{\beta}_1 x + \hat{\beta}_2 T + \hat{\beta}_3 Tx$ in red, and $y = \hat{\beta}_0 + \hat{\beta}_1 x + \hat{\beta}_2 T$ in green, where in both T = 1).

Unexpectedly, the calculated β_3, how much the effect of AAV-AD infliction depends on the baseline measurement of cognitive function (x), is estimated to be positive, meaning that the cognition deteriorating effect of AD on Y-maze score increases as average pre-AAV time increases. In other words, if a mouse was initially slower, then AAV-AD transduction led to better Y-maze performance than when compared to a mouse that was initially faster. The range of values that $(\beta_2 + \beta_3 x)$, the effect of AAV-AD infliction, can take was calculated by plugging in 0 and 120 for x as well as the estimates for the regression coefficients. Therefore, the effect of AAV-AD varies from -0.11 to 0.33. Although, β_3 appears small because of the scales of x and y, its significant effect can be seen in **Figure 14G** by the presence of the difference between the red and green lines in how the effect of AAV-AD infliction varies with x.

Table 12.

Parameter Estimate	$\widehat{\beta_0}$	$\widehat{\beta_1}$	$\widehat{\beta_2}$	$\widehat{\beta_3}$
Value	.535	-0.0012	-.111	0.0012

Table 13.

Estimate	Standard Error	p-value	95% Confidence interval
$\widehat{\beta_3}$ = 0.0012	0.0020	0.56	(-0.0028,.0.0052)

Included in Table 13 is an approximate 95% confidence interval for $\widehat{\beta_3}$, which is computed as $(\widehat{\beta_3} - 1.96 \times Standard\ error \beta_3 + 1.96 \times Standard\ error)$.

The sign of the effect of AAV-AD delivery depends on x and becomes positive for large values of x, which is contrary to the expectation that AD should make mice slower. This is saying for mice with large average pre-AAV trial times, treated mice will have higher Y-maze scores

compared to untreated mice. The p-value of the test that $\beta_3 = 0$ is 0.56, so there was no sufficient evidence from the sample to reject the null hypothesis. In other words, under the regression model, one cannot conclude that the effect of AAV-AD inoculation depends on the baseline cognitive measure of average pre-AAV Boxmaze trial time.

Boxmaze spatial learning index did not predict molecular and cellular pathologies associated with resistance to cognitive impairment by IHC.

To explore molecular changes involved across different cognition levels, immunohistochemistry technique was used for specific antigen immunodetection in the learning and memory-associated hippocampal sections of all mice brain samples. Antigen retrieval buffer enables target retrieval in formalin-fixed, paraffin-embedded tissue sections. pH of retrieval buffer in heat induced epitope retrieval (HIER) was standardized to pH 9.0 by 1X-Tris EDTA, regardless of antigen target location. Though generalized IHC steps include specimen preparation, antigen retrieval, epitope blocking, primary antibody staining, and finally detection, several execution factors determine the efficacy of the immunostaining outcome. After tissue rehydration in diluted levels of xylene and ethanol, in consideration of potential endogenous peroxidase activity present in brain tissue samples, 3% H2O2 treatment was used to prevent non-specific binding sites that might otherwise bind to the secondary antibody. Detection was performed using an HRP-conjugated secondary antibody to amplify staining intensity, followed by chromogenic detection using DAB as the substrate. For visualization, slides were dehydrated in increasing strengths of ethanol and xylene, and then mounted. Selection of Mouse or Rabbit Specific HRP/DAB Detection IHC kits (Abcam) matching complementary recognition of secondary antibody with primary antibody produced reduced cross-reactive immunoglobulin detection. Kits and reagents were kept consistent for antibody optimization, especially considering antibodies were procured from different vendors with different purification grades. To eliminate uncertainty around nonspecific binding of the secondary antibody, negative controls of brain tissue

underwent identical staining conditions minus the primary antibody. In an effort to reduce potential cross-reactivity to non-target antigens, all of the used antibodies, except one more sensitive polyclonal (PSD95), were monoclonal antibodies.

Immunohistochemistry for 3 key AD-related biomarkers was provided by services at ADRC: I6 double stained for 6E10 in brown, which recognizes β amyloid peptides, and IBA-1 in blue, which indicates resident brain macrophage microglial activation, and AT8, which recognizes phosphorylated tau proteins indicative of neurofibrillary tangles (**Figure 15A, B, C, D**). Images for processing antigen capture by DAB were taken at 20x. Because the AAV-Aβ42 viral capsid components introduced GFP reporter tags to any growths of amyloid β42, IHC for GFP antibody was conducted to substantiate localization and verify viral transduction carried correct constructs to the cell and delivered aβ42 deposition. Although the IHC stains of the fraction of AAV-Sham-given female and male mice resulted in small amounts of DAB presence, the calculated DAB OD means in these groups can be presumed to be due to background noise and are minimal compared to their AAV-AD-given counterparts (**Figure 16A**). And looking specifically at IHC stain measurements of 6E10 (**Figure 16B**), there was a shared differential expression pattern across all cohorts with GFP DAB stained sample OD distribution. For β-amyloid peptide and microglial activation for neuroinflammation, 6E10 and IBA-1 stains had strong evidence of differences between groups. Female and male AD groups had higher 6E10 detecting DAB OD means than their Sham counterparts (Predicted LS mean difference = 0.1253, p = <0.0001), (Predicted LS mean difference = 0.1854, p = <0.0001), implying AD-vector induced amyloid β development. Additionally, female and male mice given AD showed statistical significance (Predicted LS mean difference = -0.06750, p = 0.0011) For neurofibrillary tangle examination, AT8 stained brains only showed significant difference between AD Females vs. AD Males (Predicted LS mean difference = 0.06518, p=0.0008) by 2-way ANOVA post-hoc Tukey's multiple comparison test, accounting for sex and vector type (**Figure 16B**).

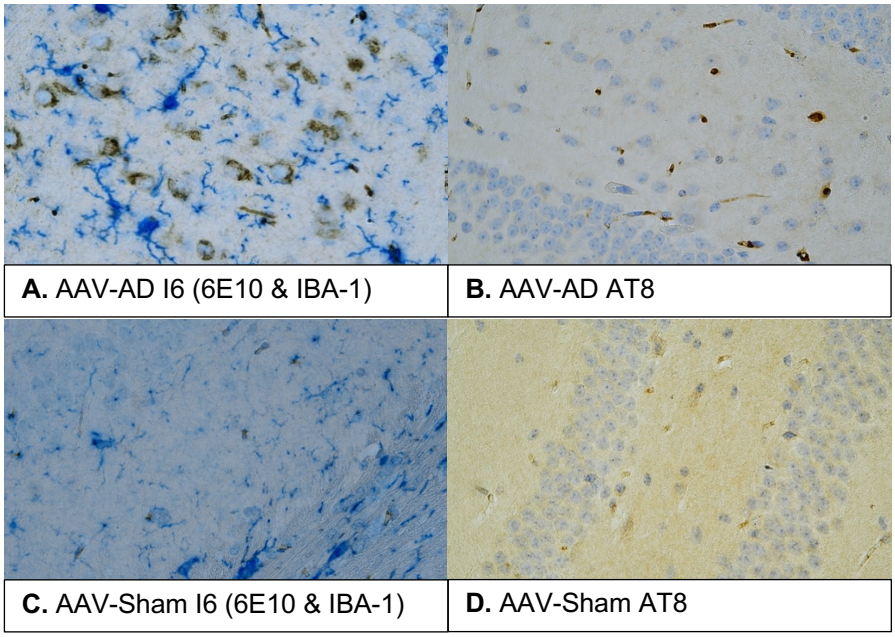

A. AAV-AD I6 (6E10 & IBA-1)	**B.** AAV-AD AT8
C. AAV-Sham I6 (6E10 & IBA-1)	**D.** AAV-Sham AT8

Figure 15. Representative image at 40x magnification of AAV-AD injected female mouse hippocampal IHC slide stain for **A.** I6 **B.** AT8 **C.** AAV-Sham injected female mouse IHC stain for I6 and **D.** AT8. I6 is a double stain for 6E10 as brown, and IBA-1 as blue.

Mice given AAV-AD treated groups were anticipated to have upregulated expression of proteins in inflammatory pathways, and synaptic structure, from genes that regulate chromatin remodeling and related epigenetic changes, and a downregulated expression of proteins that are counter-regulatory to oxidative stress (**Jiang et al., 2022**). To investigate these pathological events, the following antibodies were used for IHC on hippocampal tissue: IL-6, a cytokine associated with immune response, PSD95, a membrane-associated protein located in the postsynaptic density of neurons and marks synaptic density and changes in synaptic structure in neurological disorders, γH2AX, a histone which becomes phosphorylated at the site of DNA double-stranded breaks and marks for DNA damage and cellular repair processes, MCP-1, a chemokine that recruits immune cells to tissue trauma and indicates inflammation, and TNF-alpha, a pro-inflammatory cytokine with neurotoxic effect and triggers oxidative stress (**Figure 16C**). For all antibodies, AD Female, AD Male, Sham Female, and Sham Male groups were cross-analyzed by statistical hypothesis testing 2-Way ANOVA using post-hoc correction for

multiple comparisons by Tukey's test. The adjusted p-values for multiple comparisons for all pair-wise comparisons were statistically insignificant except for ones for TNF-alpha, where 3 comparisons showed significance: AD Female vs. AD Male (Predicted LS mean difference = 0.2164, p = <0.0001), AD Female vs. Sham Female (Predicted LS mean difference = 0.1082, p = <0.0001), Sham Female vs. Sham Male (Predicted LS mean difference=0.1285, p = <0.0001) (**Figure 16D**).

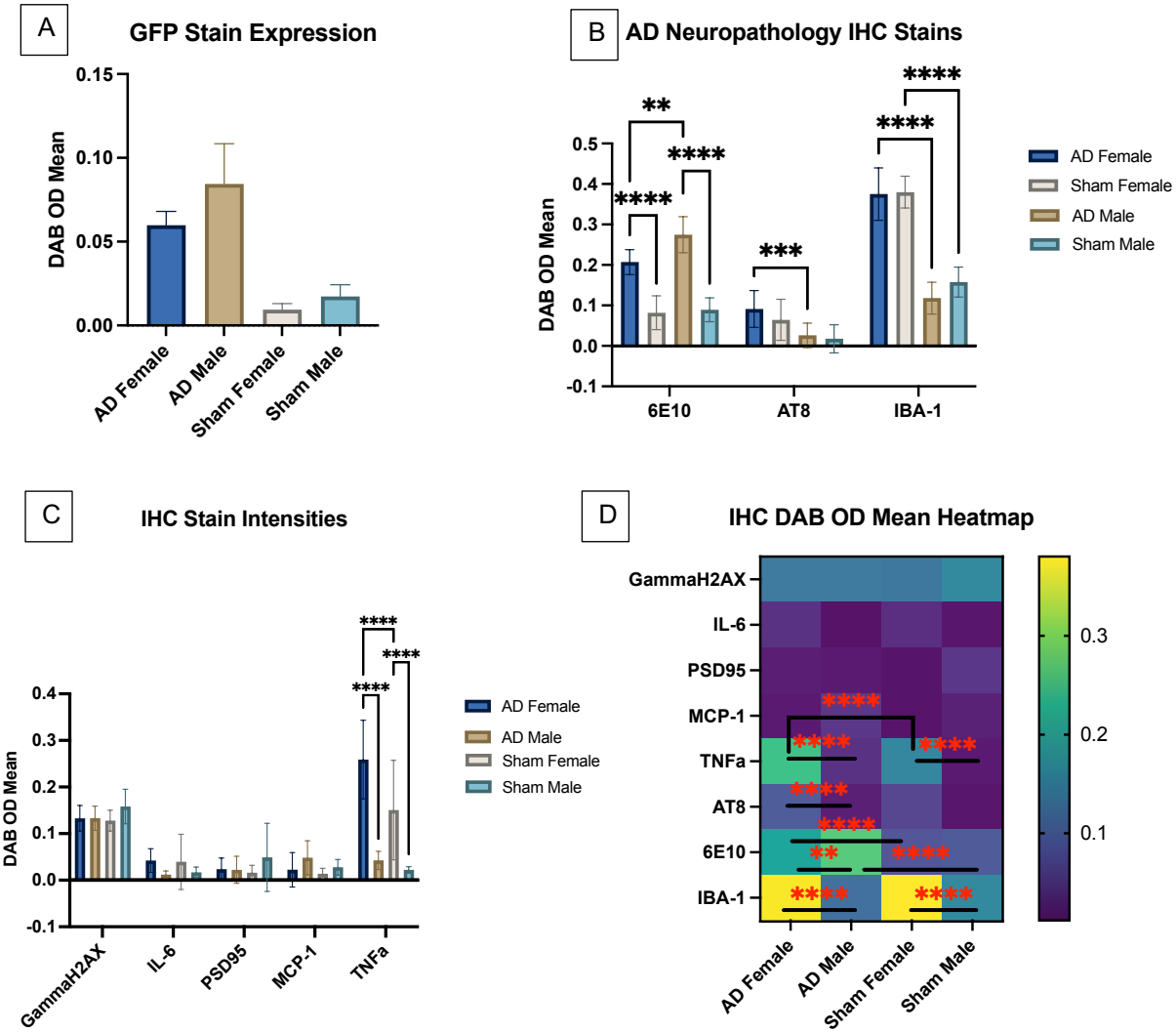

Figure 16. A. Hippocampal IHC DAB OD mean distribution for GFP antibody, reporter of AAV-AD. B. IHC DAB OD mean expression panel of AD neuropathology markers 6E10, IBA-1, AT8. **C.** IHC stains' DAB OD mean panel for γH2AX, IL-6, PSD95, MCP-1, and TNFa. **D.** Heatmap of IHC DAB OD intensities by columns representing cohort and rows representing antibody staining mean expression. Significance is set at p<0.05 and is indicated by *. N = 5-14 per cohort.

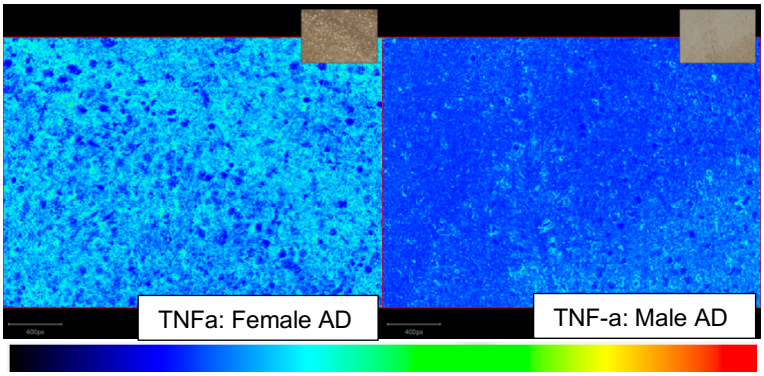

Figure 17. Representative IHC DAB OD mean expression measurement heatmaps comparing female and male AD hippocampus stained for TNF-a. Staining intensity is based on RGB color deconvoluted vector signal with dark blue suggesting lower levels, green being moderate, and red as high (Measurement mapper display min: -0.10, max: 1.0).

Correlation analysis comparing pre-AAV Boxmaze learning index with IHC staining DAB OD means for all antibodies did not show evidence of strong correlations when all cohorts were pooled; all correlations had Pearman r values <0.7. The r values were as follows: γH2AX r = 0.35, IL-6 r = 0.18, MCP-1 r = -0.09, PSD95 r = -0.23, TNFa r = 0.10, 6E10 r =-0.32, IBA-1 r = -0.07, AT8 r = 0.31 (**Figure 18A B C D E F G H**).

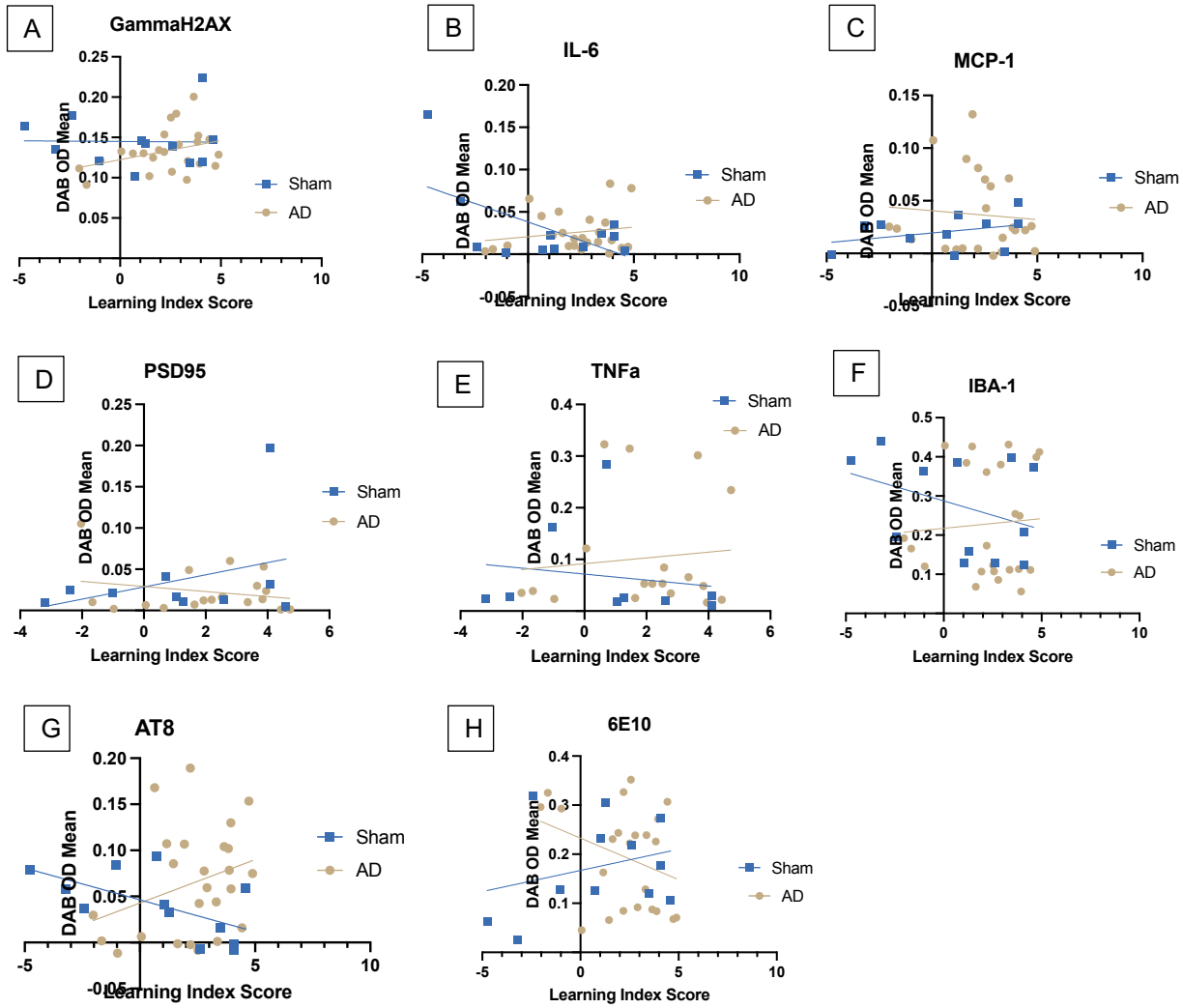

Figure 18. A. Scatter plot of γH2AX IHC DAB OD means and pre-AAV Boxmaze learning index. **B.** Scatter plot of IL-6 IHC DAB OD means and pre-AAV Boxmaze learning index. **C.** Scatter plot of MCP-1 IHC DAB OD means and pre-AAV Boxmaze learning index. **D.** Scatter plot of PSD95 IHC DAB OD means and pre-AAV Boxmaze learning index. **E.** Scatter plot of TNFa IHC DAB OD means and pre-AAV Boxmaze learning index. **F.** Scatter plot of IBA-1 IHC DAB OD means and pre-AAV Boxmaze learning index. **G.** Scatter plot of AT8 IHC DAB OD means and pre-AAV Boxmaze learning index. **H.** Scatter plot of 6E10 IHC DAB OD means and pre-AAV Boxmaze learning index. Significance is set at $p<0.05$ and is indicated by *. N=9-25 per cohort.

When the linear correlation data between Sham and AD mice were split into two regressions for each antibody inspected with IHC, a test for the difference between the slopes was done. 2-tailed t-test for the pairs of slopes between AD and Sham mice resulted in statistical difference in only two antibody biomarkers: IL-6 ($t(34) = 3.45$, $p=0.019$) and AT8 ($t(34) = 2.44$, $p=0.02$). 6E10 had a strong evidence of difference but not statistically significant ($t(34) = 1.78$, $p=0.08$). Details for all slope comparisons can be found in **Table 14**.

Table 14.

$Slope_{AD}$	$Slope_{Sham}$	Standard $Error_{(difference)}$	p-value	T estimate
γH2AX $\widehat{\beta_0} = 0.00475$	γH2AX $\widehat{\beta_0} = -0.0001$	0.000558	0.26	1.14
IL-6 $\widehat{\beta_0} = 0.00226$	IL-6 $\widehat{\beta_0} = -0.008723$	0.001167	0.019	2.45
MCP-1 $\widehat{\beta_0} = -0.0016$	MCP-1 $\widehat{\beta_0} = 0.00185$	0.002627	0.459	0.75
PSD95 $\widehat{\beta_0} = -0.0031$	PSD95 $\widehat{\beta_0} = 0.007383$	0.003813	0.179	1.37
TNFa $\widehat{\beta_0} = 0.005599$	TNFa $\widehat{\beta_0} = -0.00575$	0.00006	0.55	0.60
6E10 $\widehat{\beta_0} = -0.01692$	6E10 $\widehat{\beta_0} = 0.008627$	0.001643	0.08	1.78
IBA-1 $\widehat{\beta_0} = 0.004958$	IBA-1 $\widehat{\beta_0} = -0.01471$	0.00379	0.33	1.00
AT8 $\widehat{\beta_0} = 0.009413$	AT8 $\widehat{\beta_0} = -0.006921$	0.003179	0.02	2.44

Discussion

Cognition allows knowledge processing through thought, experience, and physical senses. It is a crucial ability for healthy aging and prevention of neurological disease onset. However, cognitive function seems to diminish with increasing age. Yet, individuals of the same age in older populations can present with varying diminished levels of cognition. Results from the Boxmaze spatial navigation test produced numerical calculations for displaying place learning and scoring cognitive function ability. The results were explored for the best way to represent, evaluate, and understand heterogeneity of age related cognitive decline across different sex and AD-resembling pathologies, and the developed representation method was used to identify molecular pathways associated with resistance to AD neuropathology in the hippocampal brain region.

The purpose of the vectors was to compare the response of the two aging-phenotypes by exacerbating the Aβ and phosphorylated Tau reactions, for best comparison of a normally aged neuropathology background to a cognitively impaired one. The expectation was that after two months, the vector transductions would evoke noticeable behavioral and pathological displays of individualistic resistance to AD disease progression. The Boxmaze escape time results would select out healthy aged mice apart from mice associated with more severe cognitive impairment, suggesting preventative factors associated with AD resistance. It was anticipated that those who showed more susceptibility to AD would have stronger manifestation of demented behaviors. This type of phenotypic cognition inhibitory effect of the AD vector was validated via the multiple linear regression model on Boxmaze (**Figure 7**), and the ROC binary classifier on the learning index (**Figure 9**). IHC using the GFP antibody showed AD-treated mice had elevated levels of DAB staining compared to their Sham counterparts, validating the proper expression of AAV-Aβ42 and its reporter gene sequence encoding for GFP (**Figure 16A**).

Indeed, the IHC DAB OD mean results for 6E10 β-amyloid expression showed a similar comparative pattern across cohorts as the GFP stained brains, reinforcing the work of the AD vector transduction in AD mice. Although AT8 antibody staining data did not show the same robustly elevated levels in DAB signaling of the pTauP301L component from AD-cohorts (**Figure 16B**), AD female mice had higher AT8 expression than Sham females, and AD males had higher AT8 expression than Sham males. The similar intensities of staining between AD and Sham cohorts indicates reason to investigate other possible cross-reacting antigen prospects in mice brains. There was a significant difference in tau expression between AD-treated males and females. The underlying pathways involved in differential taupathy must be further investigated to understand the possibility of the sex difference.

Reference memory to test learning and working memory has been studied in previous studies involving the Boxmaze assay (**Darvas et al., 2019).** And they all used different calculation approaches to analyze the data. Here, we proposed a protocol based on first-time exposure navigation ability to accomplish the Boxmaze, to decipher short-term learning in C57BL/6 mice.

The Boxmaze spatial navigation learning task produced data used to generate a sample specific learning index. The learning index scores were designed to serve as predictors to Aβ or Tau neuropathology feature development, which are key indicators of increased risk for AD. However, within the paradigm of this learning index system, rate of AD neuropathology development was not predicted (**Figure 18 F, G, H**). Still, by extension of this design, a future more intricate and robust development of the learning index, with better consideration of the scaling of cognitive impairment and AD neuropathology rates, could be applied on older individuals who are at risk to progressive cognitive impairment (**Figure 11E**) for identification of MCI susceptibility.

Animal behavioral tasks involving high or insufficient levels of stress can influence the animal's performance. Mice are nocturnal natural predatory victims and tend to hide from light and open areas which increase anxiety **(Bailey et al., 2009).** But if the Boxmaze's use of a hot light source was not ample aversive stimuli, the mice may not be encouraged to complete the maze. Rather, the mice may be acclimated enough and curious to simply explore the arena, failing to provide learning reinforcement evidence. It is important to employ different measuring parameters, not just latency, like path length to escape hole, path pattern, time spent in spaces around the maze, number of head deflection errors to the correct escape hole (otherwise known as primary errors: mice could have found the target but lacked the motivation to enter it and so then continued to explore the maze). With just using times, one cannot confirm mouse learned the association between spatial room cues and escape location. For future studies, a meta-data approach which includes the latency and number of head pokes into holes can augment the learning index system's computing power in considering the comprehensive learning nature of cognition.

Spontaneous alteration is a measure of spatial working memory and is driven by innate curiosity of rodents to explore previously unvisited areas. Mice with intact working memory will remember the arms previously visited and tend to enter a less recently visited arm (**A. K. Kraeuter, P. C. Guest, & Z. Sarnyai, 2019**). Post-AAV, spatial reference memory and cue-dependent learning was tested by Boxmaze and Y-maze respectively, to assess both cognition domains in the sample set that exemplified baseline heterogenous cognitive levels. This study showed that both types of cognition measured by Y-maze and Boxmaze, were more negatively affected by the inducement of AD than for the Sham group.

Correlation analysis tested the notion that based on the diversity in the AD-inoculated mice test results showing their demented impairment variation, whether resiliency to AD symptoms

prevails more in baseline cognitively healthy mice. There was a fair correlation between baseline cognitive levels and cue-dependent memory in an aged AD background with Spearman r=0.53, measured by Boxmaze (**Figure 11F**), while there was no sign of correlation between baseline cognitive levels and spatial working memory with Spearman r=0.141, measured by Y-maze (**Figure 13C**). However, importantly, there was no compelling statistical evidence that individualistic resilience to AD onset can predict or is confidently correlated with the rate of cognitive decline. Whether natural brain aging distinguishes mice with impaired learning from their resistant counterparts with preserved cognitive function with respect to place learning and cognitive stress parameters of Y-maze or WBC counts was not robustly validated via the Boxmaze learning index correlational analyses.

In IHC, the detection of these markers can help elucidate the pathological state of tissue, such as the presence of inflammation (MCP-1), type of inflammatory response (IL-6, TNFa, IBA-1), occurrence of DNA damage or post-synaptic development (γH2AX, PSD95), or the accumulation of characteristic protein aggregates seen in neurodegenerative diseases (6E10, AT8). The presence, absence, or quantity of these markers in specific tissue contexts can provide valuable insights into disease mechanisms and progression. Care was taken to include negative control validation for all IHC experiments and keep optimized incubation times and solution dilutions consistent. However, IHC is difficult to control for minimizing high background and non-specific binding, especially if there needs to be special consideration of the specific type of biological process and tissue sample the researcher is questioning. For example, γH2AX has cellular localization in chromosomes of the nucleus, whose membrane checks entry. Protocols advise adding permeabilizing agents such as Triton X (which was not used in this study) to the antibody dilution buffer and blocking buffer to aid antibody penetration into the nucleus. Perhaps this is why the γH2AX DAB OD data display similar vicinities of staining due to the antibody inability to bind to its true signal intensifying target antigen.

Statistically significant differences were present in IHC data between AD-female and male brains stained for IBA-1. The difference in environment sensitive microglial activation between sex in older aged mice treated with AAV-AD must be further investigated to be able to make claims about sex related resilience to AD consequences. There was a sex difference in AD-brains stained for TNFa. Interestingly, there was also a difference in female and male Sham-given brains stained for TNFa, which means there is a sex difference in TNFa levels occurring in naturally aged cognitive decline background without of AD-pathology. So it follows that there was a statistically significant difference between AD and Sham female mice. A better look at the role of TNFa in an AD background by investigating the pleiotropic regulatory functions and numerous brain signaling pathways and it is involved in, may elucidate the sex difference.

The learning index was used to compare the IHC pathological signatures that serve as biomarkers to aging. In **Figure 18**, what is interesting is that AD and Sham slopes generally seem to go in opposing directions. But looking at the distribution of data points and judging by the Spearman r correlation values, any kind of inference made on correlation of IHC DAB OD means and learning index would be very weak. Perhaps increasing sample size for added power would create a better dataset fitting or perhaps the linear model approach does not reflect the non-linear relationship between learning index scale and DAB OD means. It would be of interest to correlate the learning index with different glial cells like astrocytes and oligodendrocytes and compare these correlational data with other regions of the brain.

If cognition relies on the biological aging processes of the brain, neuropathology can be targeted for interventions that can lengthen healthy living. Phenotypic cognitive data showed that mice had differing susceptibilities to further cognitive decline which was not robustly correlated with baseline measures of cognitive function; only pre-AAV learning index and post-AAV learning index were remotely correlated. Molecular immunostaining data showed that the behavioral

phenotypes associated with cognitive impairment were not correlated with neuropathology or other inflammation or immune markers. In this study, there were no phenotypic or neuropathological features in ARCI resilience during brain aging.

References

Bailey KR, Crawley JN. Anxiety-Related Behaviors in Mice. In: Buccafusco JJ, editor. Methods of Behavior Analysis in Neuroscience. 2nd edition. Boca Raton (FL): CRC Press/Taylor & Francis; 2009. Chapter 5. Available from: https://www.ncbi.nlm.nih.gov/books/NBK5221/

Bankhead, P., Loughrey, M.B., Fernández, J.A. *et al.* QuPath: Open source software for digital pathology image analysis. *Sci Rep* **7**, 16878 (2017). https://doi.org/10.1038/s41598-017-17204-5

Benros ME, Sørensen HJ, Nielsen PR, Nordentoft M, Mortensen PB, Petersen L. The Association between Infections and General Cognitive Ability in Young Men - A Nationwide Study. PLoS One. 2015 May 13;10(5):e0124005. doi: 10.1371/journal.pone.0124005. PMID: 25970427; PMCID: PMC4429968.

Cook C, Kang SS, Carlomagno Y, Lin WL, Yue M, Kurti A, Shinohara M, Jansen-West K, Perkerson E, Castanedes-Casey M, Rousseau L, Phillips V, Bu G, Dickson DW, Petrucelli L, Fryer JD. Tau deposition drives neuropathological, inflammatory and behavioral abnormalities independently of neuronal loss in a novel mouse model. Hum Mol Genet. 2015 Nov 1;24(21):6198-212. doi: 10.1093/hmg/ddv336. Epub 2015 Aug 13. PMID: 26276810; PMCID: PMC4599677.

Darvas, M., Mukherjee, K., Lee, A., & Ladiges, W. (2020). A Novel One-Day Learning Procedure for Mice. Current Protocols In Mouse Biology, 10(1). doi: 10.1002/cpmo.68

Forner S, Martini AC, Prieto GA, Dang CT, Rodriguez-Ortiz CJ, Reyes-Ruiz JM, Trujillo-Estrada L, da Cunha C, Andrews EJ, Phan J, Vu Ha J, Chang AVZD, Levites Y, Cruz PE, Ager R, Medeiros R, Kitazawa M, Glabe CG, Cotman CW, Golde T, Baglietto-Vargas D, LaFerla FM. Intra- and extracellular β-amyloid overexpression via adeno-associated virus-mediated gene transfer impairs memory and synaptic plasticity in the hippocampus. Sci Rep. 2019 Nov 4;9(1):15936. doi: 10.1038/s41598-019-52324-0. PMID: 31685865; PMCID: PMC6828807.

Gage, F. H., Dunnett, S. B., & Björklund, A. (1984). Spatial learning and motor deficits in aged rats. *Neurobiology of Aging, 5*(1), 43–48. https://doi.org/10.1016/0197-4580(84)90084-8

Gallagher M, Burwell RD. Relationship of age-related decline across several behavioral domains. Neurobiol Aging. 1989 Nov-Dec;10(6):691-708. doi: 10.1016/0197-4580(89)90006-7. PMID: 2628781.

Hickman DL. Evaluation of the neutrophil:lymphocyte ratio as an indicator of chronic distress in the laboratory mouse. Lab Anim (NY). 2017 Jun 23;46(7):303-307. doi: 10.1038/laban.1298. PMID: 28644453; PMCID: PMC7091828.

Huang Q, Chan KY, Tobey IG, Chan YA, Poterba T, Boutros CL, Balazs AB, Daneman R, Bloom JM, Seed C, Deverman BE. Delivering genes across the blood-brain barrier: LY6A, a novel cellular receptor for AAV-PHP.B capsids. PLoS One. 2019 Nov 14;14(11):e0225206. doi: 10.1371/journal.pone.0225206. PMID: 31725765; PMCID: PMC6855452.

Jackson Laboratory. Physiological Data Summary -Aged C57BL/6J (000664).

Jang S, Shen HK, Ding X, Miles TF, Gradinaru V. Structural basis of receptor usage by the engineered capsid AAV-PHP.eB. Mol Ther Methods Clin Dev. 2022 Jul 31;26:343-354. doi: 10.1016/j.omtm.2022.07.011. PMID: 36034770; PMCID: PMC9382559.

Jiang Z, Wang J, Imai D, Snider T, Klug J, Mangalindan R, Morton J, Zhu L, Salmon AB, Wezeman J, Hu J, Menon V, Marka N, Neidernhofer L, Ladiges W. Short term treatment with a cocktail of rapamycin, acarbose and phenylbutyrate delays aging phenotypes in mice. Sci Rep. 2022 May 4;12(1):7300. doi: 10.1038/s41598-022-11229-1. PMID: 35508491; PMCID: PMC9067553.

Lawlor PA, Bland RJ, Das P, Price RW, Holloway V, Smithson L, Dicker BL, During MJ, Young D, Golde TE. Novel rat Alzheimer's disease models based on AAV-mediated gene transfer to selectively increase hippocampal Abeta levels. Mol Neurodegener. 2007 Jun 9;2:11. doi: 10.1186/1750-1326-2-11. PMID: 17559680; PMCID: PMC1906777.

Mukherjee, K., Lee, A., Zhu, L., Darvas, M., & Ladiges, W. (2019). Sleep-deprived cognitive impairment in aging mice is alleviated by rapamycin. Aging Pathobiology and Therapeutics, 1(1), 05-09.

Pedregosa, F., Varoquaux, G., Gramfort, A., Michel, V., Thirion, B., Grisel, O., ... & Duchesnay, E. (2011). Scikit-learn: Machine learning in Python. Journal of Machine Learning Research, 12(Oct), 2825-2830.

Plácido J, Ferreira JV, Araújo J, Silva FO, Ferreira RB, Guimarães C, de Carvalho AN, Laks J, Deslandes AC. Beyond the Mini-Mental State Examination: The Use of Physical and Spatial Navigation Tests to Help to Screen for Mild Cognitive Impairment and Alzheimer's Disease. J Alzheimers Dis. 2021;81(3):1243-1252. doi: 10.3233/JAD-210106. PMID: 33935093.

Rapp, P. R., Rosenberg, R. A., & Gallagher, M. (1987). An evaluation of spatial information processing in aged rats. *Behavioral Neuroscience, 101*(1), 3–12. https://doi.org/10.1037/0735-7044.101.1.3

STANDARD OPERATING PROCEDURE TITLE: Y-Maze Spontaneous Alternation Test CATEGORY: Behavioral Assay.

Swan MP, Hickman DL. Evaluation of the neutrophil-lymphocyte ratio as a measure of distress in rats. Lab Anim (NY). 2014 Aug;43(8):276-82. doi: 10.1038/laban.529. PMID: 25050728.

Tangen GG, Engedal K, Bergland A, Moger TA, Hansson O, Mengshoel AM. Spatial navigation measured by the Floor Maze Test in patients with subjective cognitive impairment, mild cognitive impairment, and mild Alzheimer's disease. Int Psychogeriatr. 2015 Aug;27(8):1401-9. doi: 10.1017/S1041610215000022. Epub 2015 Feb 3. PMID: 25644091.

Warren Ladiges & Denny Liggitt (2018) Testing drug combinations to slow aging, Pathobiology of Aging & Age-related Diseases, 8:1, DOI: 10.1080/20010001.2017.1407203

Zanco M, Plácido J, Marinho V, Ferreira JV, de Oliveira F, Monteiro-Junior R, Barca M, Engedal K, Laks J, Deslandes A. Spatial Navigation in the Elderly with Alzheimer's Disease: A Cross-Sectional Study. J Alzheimers Dis. 2018;66(4):1683-1694. doi: 10.3233/JAD-180819. PMID: 30507580.

Zenaro E, Pietronigro E, Della Bianca V, Piacentino G, Marongiu L, Budui S, Turano E, Rossi B, Angiari S, Dusi S, Montresor A, Carlucci T, Nanì S, Tosadori G, Calciano L, Catalucci D, Berton G, Bonetti B, Constantin G. Neutrophils promote Alzheimer's disease-like pathology and cognitive decline via LFA-1 integrin. Nat Med. 2015 Aug;21(8):880-6. doi: 10.1038/nm.3913. Epub 2015 Jul 27. PMID: 26214837.

Supplementary Data

Supplementary Table 1.

Weight (g)	Trial 1 (s)	Trial 2 (s)	Trial 3 (s)	Trial 4 (s)	Average (s)	Hole Entry Attempts	Pellets	Grooming Behavior
31.9	120	10	80	12	55.5	9	0	1
33.8	120	120	21	5	66.5	7	0	0
23.6	120	120	81	40	90.25	12	4	0
23.3	120	21	55	9	51.25	4	0	0
26.6	120	91	75	12	74.5	13	0	0
26	120	100	13	80	78.25	18	0	1
25.2	120	12	23	120	68.75	8	2	2
27.8	71	18	87	120	74	9	0	1
25.7	112	25	18	41	49	16	3	1
30.1	116	104	120	120	115	13	2	3
27	30	89	120	120	89.75	7	1	0
33.7	97	21	31	68	54.25	14	1	0
33.9	30	53	78	9	42.5	7	3	0
29.5	84	27	40	120	67.75	12	2	0
39.1	63	89	120	120	98	18	0	1
33	89	22	120	93	81	22	0	0
29.3	120	120	58	114	103	14	1	1
27.1	78	9	104	94	71.25	5	2	0
27.9	69	13	102	120	76	22	2	1
36.09	120	120	76	58	93.5	17	1	0
32.38	120	29	35	75	64.75	18	0	1
27.29	120	88	6	43	64.25	13	0	0
29.32	120	75	120	74	97.25	19	4	0
32.14	120	35	38	92	71.25	9	0	0
29.47	120	120	65	37	85.5	13	0	1
35.2	120	76	15	45	64	3	0	1
33.81	120	45	120	120	101.25	11	2	2
33.17	30	14	13	81	34.5	8	0	0
31.92	120	112	120	72	106	21	0	2
32.79	30	5	60	52	36.75	10	0	0
30.43	120	68	120	51	89.75	14	0	2
35.12	69	50	104	84	76.75	21	0	0
36.91	120	15	68	27	57.5	12	0	0
33.55	67	14	97	12	47.5	8	0	1
37.37	98	35	84	55	68	15	0	1
34.12	120	55	42	32	62.25	12	1	0

35.02	120	112	56	38	81.5	4	1	0
31.59	44	77	107	5	58.25	9	0	0
33.29	71	10	18	45	36	4	0	0

Supplementary Table 2.

Mouse ID	Sex	Vector Type	Learning Index Score (Pre-AAV)	Learning Index Score (Post-AAV)
MCI-1 LF	Female	SHAM	4.59567602	1.80062417
MCI-1 RF	Female	AD	3.87523056	0.60829469
MCI-1 LB	Female	AD	2.18906917	2.29807258
MCI-1 RB	Female	AD	4.89158045	1.8115152
MCI-2 LF	Female	AD	3.3145162	2.14085453
MCI-2 RF	Female	AD	2.91627077	0.5757509
MCI-2 LB	Female	SHAM	3.46693968	1.06911333
MCI-2 RB	Female	SHAM	NA	NA
MCI-3 LF	Female	AD	4.7330252	1.78318217
MCI-3 RF	Female	AD	0.06014083	0.83353159
MCI-4 LF	Female	SHAM	-16.9608016	0.55644594
MCI-4 RF	Female	AD	3.6557461	0.81467781
MCI-4 LB	Female	SHAM	-3.2050127	-2.4443432
MCI-4 RB	Female	AD	1.45768107	1.39900496
MCI-5 LF	Female	SHAM	-4.7500429	-0.6192643
MCI-5 RF	Female	SHAM	0.71136644	1.13914816
MCI-5 LB	Female	AD	1.16639987	2.43727149
MCI-6 LB	Female	AD	0.64159532	1.04461116
MCI-6 RB	Female	SHAM	-1.0246969	0.95442191
MCI-7 LF	Male	AD	1.93022435	0
MCI-7 RF	Male	AD	3.83584594	2.49436896
MCI-7 NP	Male	AD	3.94383005	NA
MCI-8 LB	Male	AD	1.63715101	1.11542915
MCI-8 RB	Male	AD	3.35918814	2.17261382
MCI-8 NP	Male	AD	2.51779098	1.33660437
MCI-9 LF	Male	AD	3.9553258	1.87828545
MCI-9 RF	Male	SHAM	1.26480172	0.84171548
MCI-9 NP	Male	AD	-1.6620048	-1.4925167
MCI-10 LB	Male	SHAM	1.05136781	1.1429371
MCI-10 RB	Male	AD	-2.0295914	1.30432073

MCI-10 NP	Male	AD	2.19433416	0.19906552
MCI-11 LF	Male	AD	-0.9734926	1.78159575
MCI-11 RF	Male	AD	4.42854602	2.40770394
MCI-11 LB	Male	AD	2.57004604	0.7637645
MCI-11 RB	Male	SHAM	2.59706677	0.94990874
MCI-12 LF	Male	SHAM	4.09961639	2.00859572
MCI-12 LB	Male	AD	2.78629721	2.81581966
MCI-12 RF	Male	SHAM	-2.4019109	-0.6183434
MCI-12 RB	Male	SHAM	4.09736603	1.21688693

Supplementary Table 3.

Table Analyzed	post infection learning index
Column B	Female Sham
vs.	vs.
Column A	Female AD
Mann Whitney test	
P value	0.1259
Exact or approximate P value?	Exact
P value summary	ns
Significantly different (P < 0.05)?	No
One- or two-tailed P value?	Two-tailed
Sum of ranks in column A,B	122 , 49
Mann-Whitney U	21
Difference between medians	
Median of column A	1.399, n=11
Median of column B	0.9544, n=7
Difference: Actual	-0.4446
Difference: Hodges-Lehmann	-0.8288

Supplementary Table 4.

Table Analyzed	post infection learning index
Column D	Male Sham
vs.	vs.
Column C	Male AD
Mann Whitney test	
P value	0.3676
Exact or approximate P value?	Exact
P value summary	ns
Significantly different (P < 0.05)?	No
One- or two-tailed P value?	Two-tailed
Sum of ranks in column C,D	141 , 49

Mann-Whitney U	28
Difference between medians	
Median of column C	1.337, n=13
Median of column D	1.046, n=6
Difference: Actual	-0.2902
Difference: Hodges-Lehmann	-0.4742

Supplementary Table 5.

Table Analyzed	Learning index (by pre and post)
Column B	Post-AAV
vs.	vs.
Column A	Pre-AAV
Wilcoxon matched-pairs signed rank test	
P value	0.0884
Exact or approximate P value?	Exact
P value summary	ns
Significantly different (P < 0.05)?	No
One- or two-tailed P value?	Two-tailed
Sum of positive, negative ranks	238.0 , -465.0
Sum of signed ranks (W)	-227.0
Number of pairs	37
Number of ties (Pratt's method)	0
Median of differences	
Median	-1.174
How effective was the pairing?	
rs (Spearman)	0.5311
P value (one tailed)	0.0004
P value summary	***
Was the pairing significantly effective?	Yes

Supplementary Table 6.

ANOVA table	SS	DF	MS	F (DFn, DFd)	P value
Female vs. Male	1790630039	1	1790630039	F (1, 29) = 10.65	P=0.0028
Pre-AAV vs. Post-AAV	68856287	1	68856287	F (1, 29) = 0.4096	P=0.5272
AD vs. Sham	355979431	1	355979431	F (1, 29) = 2.814	P=0.1042
Female vs. Male x Pre-AAV vs. Post-AAV	1666034	1	1666034	F (1, 29) = 0.009911	P=0.9214
Female vs. Male x AD vs. Sham	562150974	1	562150974	F (1, 29) = 4.444	P=0.0438
Pre-AAV vs. Post-AAV x AD vs. Sham	32565264	1	32565264	F (1, 29) = 0.2574	P=0.6157

Supplementary Table 7.

Šídák's multiple comparisons test	Predicted (LS) mean diff.	95.00% CI of diff.	Below threshold?	Summary	Adjusted P Value
Female:AD Pre-AAV vs. Male:AD Pre-AAV	-4952	-20139 to 10236	No	ns	0.9927
Female:AD Post-AAV vs. Male:AD Post-AAV	-18492	-33679 to -3305	Yes	**	0.0074
Female:Sham Pre-AAV vs. Male:Sham Pre-AAV	-5681	-30597 to 19235	No	ns	0.9998
Female:Sham Post-AAV vs. Male:Sham Post-AAV	-19238	-44154 to 5678	No	ns	0.2642
Female:AD Pre-AAV vs. Female:AD Post-AAV	3010	-12588 to 18608	No	ns	>0.9999
Female:Sham Pre-AAV vs. Female:Sham Post-AAV	-242.9	-18886 to 18401	No	ns	>0.9999
Male:AD Pre-AAV vs. Male:AD Post-AAV	-10531	-24211 to 3150	No	ns	0.2503
Male:Sham Pre-AAV vs. Male:Sham Post-AAV	-13800	-42279 to 14679	No	ns	0.8446
Female:AD Pre-AAV vs. Female:Sham Pre-AAV	-375.7	-18169 to 17418	No	ns	>0.9999
Female:AD Post-AAV vs. Female:Sham Post-AAV	-3629	-21422 to 14165	No	ns	>0.9999
Male:AD Pre-AAV vs. Male:Sham Pre-AAV	-1105	-24232 to 22021	No	ns	>0.9999
Male:AD Post-AAV vs. Male:Sham Post-AAV	-4374	-27501 to 18752	No	ns	>0.9999

Supplementary Table 8. (NLR 3-way ANOVA)

ANOVA table	SS	DF	MS	F (DFn, DFd)	P value
Female vs. Male	0.5248	1	0.5248	F (1, 34) = 11.88	P=0.0015
Pre vs. Post	0.01166	1	0.01166	F (1, 34) = 0.2640	P=0.6107
Sham vs. AD	0.004438	1	0.004438	F (1, 34) = 0.1098	P=0.7424
Female vs. Male x Pre vs. Post	0.08987	1	0.08987	F (1, 34) = 2.034	P=0.1629
Female vs. Male x Sham vs. AD	0.003948	1	0.003948	F (1, 34) = 0.09772	P=0.7565
Pre vs. Post x Sham vs. AD	0.0003112	1	0.0003112	F (1, 34) = 0.007702	P=0.9306

Supplementary Table 9. (NLR 3-Way ANOVA)

Šídák's multiple comparisons test	Predicted (LS) mean diff.	95.00% CI of diff.	Below threshold?	Summary	Adjusted P Value

Female:Sham Pre-AAV vs. Male:Sham Pre-AAV	-0.1757	-0.5140 to 0.1626	No	ns	0.8100
Female:Sham Post-AAV vs. Male:Sham Post-AAV	-0.3218	-0.6601 to 0.01656	No	ns	0.0744
Female:AD Pre-AAV vs. Male:AD Pre-AAV	-0.2067	-0.4517 to 0.03834	No	ns	0.1663
Female:AD Post-AAV vs. Male:AD Post-AAV	0.0004336	-0.2446 to 0.2455	No	ns	>0.9999
Female:Sham Pre-AAV vs. Female:Sham Post-AAV	0.08494	-0.2442 to 0.4140	No	ns	0.9989
Female:AD Pre-AAV vs. Female:AD Post-AAV	-0.08310	-0.3456 to 0.1794	No	ns	0.9931
Male:Sham Pre-AAV vs. Male:Sham Post-AAV	-0.06115	-0.4166 to 0.2943	No	ns	>0.9999
Male:AD Pre-AAV vs. Male:AD Post-AAV	0.1240	-0.1087 to 0.3567	No	ns	0.7590
Female:Sham Pre-AAV vs. Female:AD Pre-AAV	-0.01502	-0.3091 to 0.2790	No	ns	>0.9999
Female:Sham Post-AAV vs. Female:AD Post-AAV	-0.1831	-0.4771 to 0.1110	No	ns	0.5813
Male:Sham Pre-AAV vs. Male:AD Pre-AAV	-0.04601	-0.3428 to 0.2507	No	ns	>0.9999
Male:Sham Post-AAV vs. Male:AD Post-AAV	0.1392	-0.1576 to 0.4359	No	ns	0.8931